Report No. FHWA-KS-16-05 ▪ FINAL REPORT▪ July 2016

Acoustic Emission Monitoring on Fiber Reinforced Bridge Panels

James Christopher Flannigan
Youqi Wang, Ph.D.

Kansas State University Transportation Center

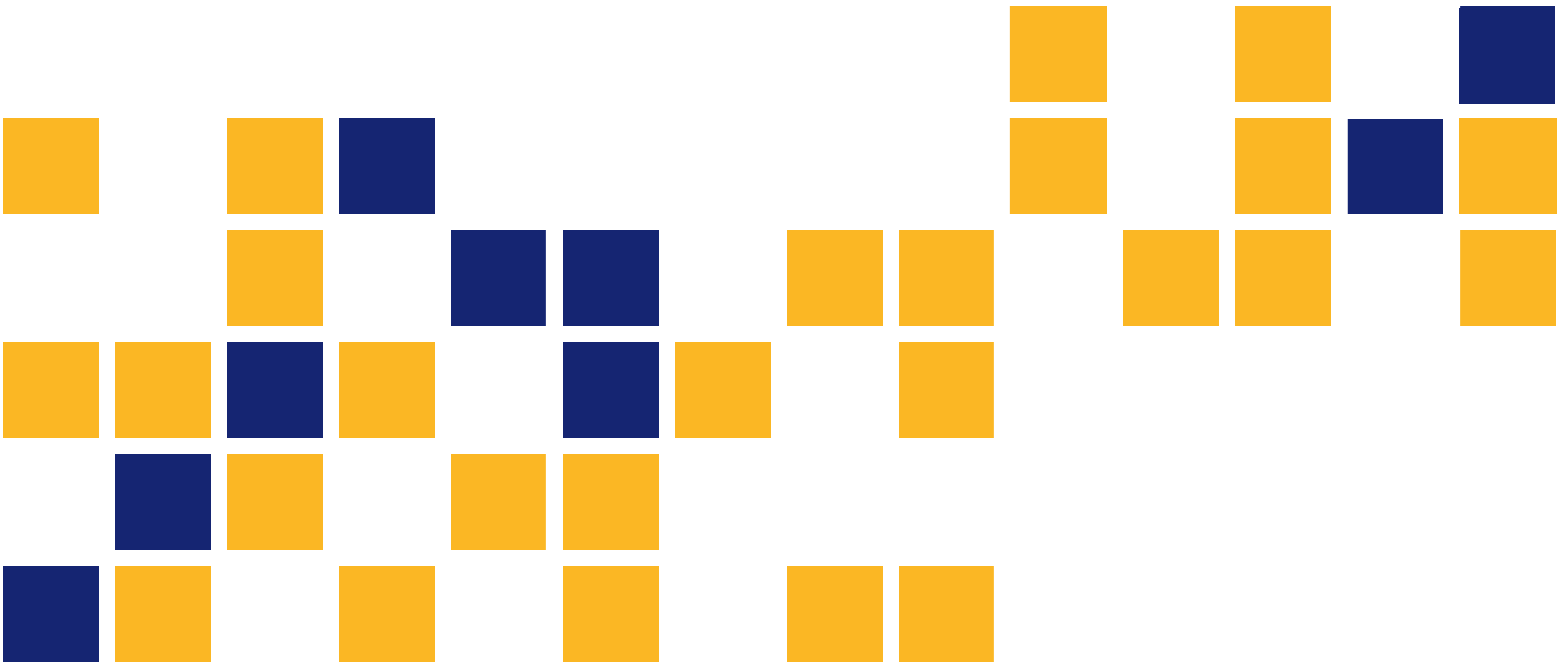

Kansas Department of Transportation

1 Report No. FHWA-KS-16-05	**2 Government Accession No.**	**3 Recipient Catalog No.**
4 Title and Subtitle Acoustic Emission Monitoring on Fiber Reinforced Bridge Panels		**5 Report Date** July 2016 **6 Performing Organization Code**
7 Author(s) James Christopher Flannigan, Youqi Wang, Ph.D.		**7 Performing Organization Report No.**
9 Performing Organization Name and Address Kansas State University Department of Mechanical and Nuclear Engineering 3002 Rathbone Hall Manhattan, KS 66506		**10 Work Unit No. (TRAIS)** **11 Contract or Grant No.** C1644
12 Sponsoring Agency Name and Address Kansas Department of Transportation Bureau of Research 2300 SW Van Buren Topeka, Kansas 66611-1195		**13 Type of Report and Period Covered** Final Report July 2006–June 2012 **14 Sponsoring Agency Code** RE-0452-01
15 Supplementary Notes For more information write to address in block 9.		

Two fiber-reinforced polymer (FRP) bridge deck specimens were analyzed by means of acoustic emission (AE) monitoring during loading cycles performed at various locations on the composite sandwich panels' surfaces. These panels were subjected to loads that were intended to test their structural response and characteristics without exposing them to a failure scenario. This allowed the sensors to record multiple data sets without fear of having to be placed on multiple panels that could have various characteristics that alter the signals recorded.

The objective throughout the analysis was to determine how the acoustic signals respond to the loading cycles and how various events could affect the acoustical data. In the process of performing this examination several steps were taken, including threshold application, data collection, and sensor location analysis. The thresholds are important for lowering the size of the files containing the data, while keeping important information that could determine structurally significant information. Equally important is figuring out where and how the sensors should be placed on the panels in relation to other sensors, panel features, and supporting beams.

The data was subjected to analysis involving the response to applied loads, joint effects, and failure analysis. Using previously developed techniques, the information gathered was also analyzed in terms of what type of failure could be occurring within the structure itself. This ability greatly helped during an unplanned failure event and the subsequent analysis to determine what may have led to the occurrence.

The basic analyses were separated into four sets, starting with the basic analysis to determine basic correlations to the loads applied. This was followed by joint and sensor location analyses, both of which took place using a two-panel setup. The last set was created upon matrix failure of the panel and the subsequent investigation.

17 Key Words Acoustic Emission, Fiber Reinforced Polymer, Failure Analysis, Sensor Data Collection		**18 Distribution Statement** No restrictions. This document is available to the public through the National Technical Information Service www.ntis.gov.	
19 Security Classification (of this report) Unclassified	**20 Security Classification (of this page)** Unclassified	**21 No. of pages** 82	**22 Price**

Form DOT F 1700.7 (8-72)

This page intentionally left blank.

Acoustic Emission Monitoring on Fiber Reinforced Bridge Panels

Final Report

Prepared by

James Christopher Flannigan
Youqi Wang, Ph.D.

Kansas State University Transportation Center

A Report on Research Sponsored by

THE KANSAS DEPARTMENT OF TRANSPORTATION
TOPEKA, KANSAS

and

KANSAS STATE UNIVERSITY TRANSPORTATION CENTER
MANHATTAN, KANSAS

July 2016

NOTICE

The authors and the state of Kansas do not endorse products or manufacturers. Trade and manufacturers names appear herein solely because they are considered essential to the object of this report.

This information is available in alternative accessible formats. To obtain an alternative format, contact the Office of Public Affairs, Kansas Department of Transportation, 700 SW Harrison, 2nd Floor – West Wing, Topeka, Kansas 66603-3745 or phone (785) 296-3585 (Voice) (TDD).

DISCLAIMER

The contents of this report reflect the views of the authors who are responsible for the facts and accuracy of the data presented herein. The contents do not necessarily reflect the views or the policies of the state of Kansas. This report does not constitute a standard, specification or regulation.

Abstract

Two fiber-reinforced polymer (FRP) bridge deck specimens were analyzed by means of acoustic emission (AE) monitoring during loading cycles performed at various locations on the composite sandwich panels' surfaces. These panels were subjected to loads that were intended to test their structural response and characteristics without exposing them to a failure scenario. This allowed the sensors to record multiple data sets without fear of having to be placed on multiple panels that could have various characteristics that alter the signals recorded.

The objective throughout the analysis was to determine how the acoustic signals respond to the loading cycles and how various events could affect the acoustical data. In the process of performing this examination several steps were taken, including threshold application, data collection, and sensor location analysis. The thresholds are important for lowering the size of the files containing the data, while keeping important information that could determine structurally significant information. Equally important is figuring out where and how the sensors should be placed on the panels in relation to other sensors, panel features, and supporting beams.

The data was subjected to analysis involving the response to applied loads, joint effects, and failure analysis. Using previously developed techniques, the information gathered was also analyzed in terms of what type of failure could be occurring within the structure itself. This ability greatly helped during an unplanned failure event and the subsequent analysis to determine what may have led to the occurrence.

The basic analyses were separated into four sets, starting with the basic analysis to determine basic correlations to the loads applied. This was followed by joint and sensor location analyses, both of which took place using a two-panel setup. The last set was created upon matrix failure of the panel and the subsequent investigation.

Acknowledgements

I would like to acknowledge Professor Youqi Wang, PhD, Kansas State University, Engineer Dave Meggers of the Kansas Department of Transportation, and technician Travis Hirt for their help and guidance on this project. I especially want to thank Richard Gostautas, who helped in several ways, including setting up our monitoring device.

Also special thanks to Kansas Structural Composites for creating and providing the FRP panels, Physical Acoustics for building the monitoring device, and the Kansas Department of Transportation and the Federal Highway Administration for sponsoring the research.

Table of Contents

Abstract v
Acknowledgements vi
Table of Contents vii
List of Figures viii
Chapter 1: Introduction 1
Chapter 2: Literature Review 7
2.1 Acoustic Emission Monitoring 7
2.1.1 Origin of Acoustic Emission Monitoring 8
2.1.2 Benefits of Acoustic Emission Monitoring 10
2.2 Acoustic Emission Monitoring on Classic Bridge Structures 12
2.3 Acoustic Emission Monitoring in Fiber-Reinforced Panels 15
Chapter 3: Experimental Method & Analysis 17
3.1 Project Stage Background 17
3.2 Equipment and Software 20
3.2.1 Equipment 20
3.2.2 Software 21
3.2.3 FRP Construction and Test Setup 23
3.2.4 Thresholds 27
3.3 Signal Distribution in Single FRP Panels 33
3.3.1 Basic Analysis of Single Panel Load Response 34
3.3.2 Single Panel Acoustic Dispersion Analysis 36
3.4 Acoustic Degradation Analysis 43
3.5 Signal Transfer in FRP Panels 50
3.6 Single Panel Failure Event Analysis 56
3.6.1 A Single Panel Analysis: Leading to Failure 56
3.6.2 Panel Failure 58
3.7 Long-Term Monitoring 62
Chapter 4: Summary and Future of Research 64
4.1 Summary 64
4.2 Future Work 66
References 68

List of Figures

Figure 1.1: No-Name Creek FRP Bridge 2
Figure 1.2: Material Delamination in Bridge Panel 5
Figure 2.1: Acoustic Wave Propagation from Failure Point, P, to Three Sensor Locations: S-1, S-2, and S-3 7
Figure 2.2: Fred Hartman Bridge 14
Figure 3.1: Load Application in Keiser Effect Analysis 18
Figure 3.2: Cross Plot of Duration versus Amplitude 19
Figure 3.3: System Enclosure and Laptop PC at Testing Site 20
Figure 3.4: Panel-A on Testing Platform 24
Figure 3.5: Close-Up of Lip-and-Groove Connection Between Two Panels 24
Figure 3.6: Bridge Deck and Support Beam Relation 25
Figure 3.7: Pneumatic Cylinder and Distribution Pad 26
Figure 3.8: Threshold Sensor Arrangement 28
Figure 3.9: Initial Analysis on an Amplitude versus Time Scale 29
Figure 3.10: 35 Decibel Amplitude Filter Comparison 30
Figure 3.11: Energy Comparison of 35 dB Amplitude and 60 Energy Count Filter 31
Figure 3.12: Amplitude Comparison of 35 dB Amplitude and 60 Energy Count Filter 31
Figure 3.13: Amplitude Comparison of 35 dB Amplitude and 85-Energy Count Filter 32
Figure 3.14: Change in Hit Number by Applying 35-Amplitude and 60-Energy Filters 33
Figure 3.15: Initial Test, Amplitude with Force Overlay 35
Figure 3.16: Energy Response with Load Overlay 36
Figure 3.17: Signal Strength Response with Load Overlay 36
Figure 3.18: Signal Dispersion Sensor Arrangement 37
Figure 3.19: Absolute Energy Values Across Sensor Array 1 38
Figure 3.20: Number of Hits Across Sensor Array 1 39
Figure 3.21: Number of Hits Across Sensor Array 1; Between 5 and 25 Kips 39
Figure 3.22: Number of Hits, Sensor Array 1; Three Tests Under 25 kips 40
Figure 3.23: Number of Hits, Sensor Array 1; Three Tests, Over 25 kips 40
Figure 3.24: Absolute Energy Values Sensor Array 1; Three Tests 41
Figure 3.25: Amplitude Values Sensor Array 1 and 2 42
Figure 3.26: Number of Hits Across Sensor Array 1 and 2 43

Figure 3.27: Average Absolute Energy Plotted at Various Sensor Distances 44
Figure 3.28: Amplitude Plotted at Various Sensor Distances..... 45
Figure 3.29: Degrading Signal Sensor Arrangement..... 46
Figure 3.30: Duration and Amplitude Comparison of Sensors; S1 and S11 47
Figure 3.31: Duration and Amplitude Comparison of Sensors; S9 and S10 48
Figure 3.32: Duration and Amplitude Comparison of Sensors; S7 and S8 49
Figure 3.33: Duration and Amplitude Comparison of Sensors; S5 and S6 50
Figure 3.34: Signal Transfer Sensor Arrangement 51
Figure 3.35: Absolute Energy Comparison of Sensors Located Equidistant from the Source; S7 On Top of Panel-A and S10 On Bottom of Panel-B..... 53
Figure 3.36: Signal Strength Comparison of Sensors Located Equidistant from the Source; S7 On Top of Panel-A and S10 On Bottom of Panel-B..... 53
Figure 3.37: Amplitude, Absolute Energy, and Signal Strength Comparison of Sensors Located Equidistant From the Source; S11 On Panel-A and S13 On Panel-B..... 54
Figure 3.38: Signal Strength Comparison of Sensors Located Equidistant From the Source; S3 and S8 On Panel-A and S15 On Panel-B..... 55
Figure 3.39: Final Sensor Location Layout 56
Figure 3.40: Test Over Beam 3, Duration-Amplitude Graph 57
Figure 3.41: Duration-Amplitude Graph of Test on the Joint Edge Between Beams 2 and 3..... 58
Figure 3.42: Failure During Test, Amplitude with Load Overlay 59
Figure 3.43: Failure During Test, Absolute Energy with Load Overlay 59
Figure 3.44: Failure During Test, Duration with Load Overlay..... 60
Figure 3.45: Duration-Amplitude Plot of the Failure Test 61
Figure 3.46: Pre- and Post-Failure Duration-Amplitude Plot of the Failure Test 62
Figure 3.47: Monitoring System’s Power and Data Flow Chart 63

This page intentionally left blank.

Chapter 1: Introduction

Interest in using fiber-reinforced polymer (FRP) as a highway bridging material began in 1970s China, with the goal of building large span, two-lane bridges. After much research and development, the world saw its first bridge deck built in Beijing, China, in 1982 (Feng, Ye, Li, & Ma, 2006). However, following this milestone in bridge design and construction, the use of composites as a serious bridging material went primarily undeveloped and no new structures are known to have been built for over a decade.

In 1993, the western-world saw its first advanced composite bridge built in Aberfeldy, Perth, and Kinross, Scotland, with decks and structural towers constructed out of E-Glass fiber material, while the support cables are made of Kevlar-49 material. These two uses resulted in not only a composite bridge, but the first to employ multiple types of composite materials in the design (BRE and Trend 2000 Ltd., 2001). However, while it met all the criteria for being a traffic bridge, it was only built to serve as a footbridge, limited to pedestrian use at the city's local golf club. The next bridge designed to carry automotive traffic is called the Bonds Mill Lift Bridge located in Stonehouse, England. While it is not a long bridge, it was the first FRP bridge outside China built specifically for vehicular traffic and is not a conventionally designed static bridge, but is instead designed as a bascule-style bridge that does not impede the active water-route it passes over. However, the overall capabilities of this structure are somewhat limited, as only a single lane of traffic is able to travel at a time and it is constantly monitored due to its untested type of material to ensure safety (McWilliam, 1994).

The first FRP bridge in the United States, and first in the western hemisphere to allow free flows of two-lane traffic, was built by Kansas Structural Composites Inc. (KSCI) in 1996 to cross No-Name Creek near Russell, Kansas. While not technically the first bridge of its kind, the advancements in design and the material's relatively new type of construction won it overwhelming praise from a variety of sources. Organizations ranging from the scientific community to the media broadcasters quickly praised it as one of the biggest advancements of its kind in several years. The accolades included the awarding of both "Best of Market" and the prestigious "Counterpoise Grand Design Award" from the International Composite Expo held in

January of 1997, as well as being recognized at the R&D 100 Awards for being one of the most important developments made that year.

Figure 1.1: No-Name Creek FRP Bridge
Source: Kansas Structural Composites, Inc. (2007)

Since installation and construction of the No-Name Creek bridge 20 years ago, several other bridges have been built by KSCI in a variety of locations. While a majority of these are in Kansas, nearly a dozen are in other states, including Missouri, New York, and West Virginia. Several other companies started up similar construction methods during this time period as well, resulting in a variety of FRP bridges across the country. The reasons for this increased interest in this construction method are numerous, and while some could be a response to civic and state governments simply wanting a new and unique structure, there are more than enough advantages to merit construction of an FRP bridge.

Fiber-reinforced polymer bridges can be installed in a relatively short amount of time. The structure itself is built at a controlled facility separate from the onsite location, making it easier to control the fabrication process as well as create parts that might be impossible to do at the construction location due to area constraints of machinery availability. Because much of the process occurs before the main construction begins, the composite material is given time to cure

and become usable as a solid panel for the bridge decks. The quick onsite installation was able to make the entire construction time of the No-Name Creek Bridge only a single day from start to finish. Adding to the ease and quickness of the construction is the relative lightness of the FRP panels in comparison to other materials, such as concrete, steel, and wood.

The decrease in panel weight also relieves much of the stress experienced by the support structure. When bridges are constructed, a large percentage of the structure is already needed to simply keep the panels in place; this can be an arduous task when the panels themselves create a large portion of the weight experienced by the structure. However, FRP panels are designed to hold a large load while remaining relatively light; the resulting lower panel dead load subsequently creates a large difference between what is and what can be loaded, increasing the amount of traffic load possible on the bridge structure.

Repairs are also capable with FRP panels if the need should arise. If there is a possibility the bridge will need widening in the future, the initial installation can be performed in a way to allow the panels to be removed and for new, larger ones to be installed quickly. The new panels can take advantage of the pre-existing support structure as well, resulting in only hours of actual construction taking place. Of course if a panel fails or starts showing signs of impending failure, it could also be replaced with another panel in a short amount of time (Kansas Structural Composites, Inc., 2007).

At the time of implementation, the No-Name Creek Bridge was new and experimental, an idea that required early research and analyses to be performed to verify the potential for future installations. To do this, a collaborative effort was initiated between Kansas State University and KSCI to determine what effects large forces have on the panels and material properties by performing both in-lab and field tests. The lab tests consisted of both small scale and full scale panel tests using static loads to record the bending properties of the material. Upon completion of the bridge, further examinations were performed; once after installation, after 1 year of service, and after 8 years of service. The post-installation analyses consisted of static loads applied by use of a dump truck at the center of each panel, slow-speed static tests, and high-speed dynamic tests in which the truck was driven over the bridge. After 8 years, the tests reported that no noticeable

change had occurred in the bridge rigidity properties, nor was it affected by environmental decay (Zhou, Wang, Meggers, & Plunkett, 2007).

Another test was conducted over the course of a year which consisted of a monitoring device measuring the temperature of the FRP panels at various points and the overall deflection of the panels. The initial analysis of this bridge was carried out by using thermal and deflection monitoring techniques to examine local climate impact on the structure over a year. The results showed that throughout the day over the course of the year, the panels follow a cyclic deflection pattern indicating that the temperature changes have a dramatic effect on the curvature of the panels. As a result there was a concern of possible delamination and eventual panel failure due to bending effects (Liu, Zhou, & Wang, 2012).

In 1999, a pair of bridges was installed on K-126 in Crawford County by the Kansas Department of Transportation (KDOT) to replace two state highway structures with significantly deteriorated decks. In the course of replacing the panels, it was necessary to widen the bridge and replace the entire deck structure with fiber-reinforced polymers (Kansas Structural Composites, Inc., 2007). Over time, the FRP panels began to delaminate between the structural face and the primary core structure. The primary cause of this occurrence is believed to have been due to the thin, flat outer material and its inability to completely bond with the core material. In Figure 1.2, the delamination occurrence between layers is quite visible upon removal of the structural face. To fix the problem, the structural face was removed, three layers of chop strain mat fiber were installed, and the structural face replaced. This created a better bond between the structural face and the core, and the bridge has now been in service to date without additional problems (D. Meggers, interview, 2016).

Figure 1.2: Material Delamination in Bridge Panel
Source: D. Meggers

Due to the possibility of the material experiencing fiber breakage or delamination, it was decided that a system should be developed to monitor FRP bridges to evaluate the potential failure of components or bond lines. A method was sought to help understand the failure mechanisms experienced by the panels when critical loads are reached. From this information, it might be possible to determine where and when a failure would occur based on sudden events and changes that happen prior to a critical break. The use of non-destructive tests (NDTs) offered highly attractive options as they would allow for monitoring of the structure while allowing the bridge to be in use. The technique decided on was acoustic emissions (AE) monitoring. This will take advantage of the sound created when a fiber breaks, layers delaminate, or other types of failures occur in most composite materials before larger failures occur. Use of this method would not require a person to be constantly present to monitor the site, and the analyzing itself can be carried out in a variety of ways, including periodic testing or continuous monitoring, allowing year-round analysis of acoustic signals and development of possible warning signs of failure.

For a proper monitoring system, a series of analyses need to be conducted to determine the proper application of AE in reference to the current project. The following points were identified as needing to be analyzed and understood before implementation of the AE monitoring device can be properly used:

1. The relationships, if any, between loading damage and the acoustic emissions detected by the sensing equipment.
2. If and what thresholds should be applied to the equipment to record data that is important for the analysis procedure while removing background and environmental noise.
3. Determine the range that should be used for the sensors in terms of the area each can cover functionally and the distance they can be placed from each other.
4. Possible sensor arrangements and placement constraints that should be used in future analyses.
5. Possible sensor layout for long-term monitoring analysis.

Chapter 2: Literature Review

The possible applications for acoustic emissions are obvious in the field of bridge structures, and there are many possibilities within the field of composite structures. The following is a review of the history and development of acoustic emission monitoring, as well as related modern uses. It is important to examine what exactly these emissions are, as well as get a brief look into the history behind this subject and how it developed into what it is today. In this section, the development of past uses and some current applications of acoustic emission monitoring will be presented to explain the background of acoustic emissions and where it could be used in the future.

2.1 Acoustic Emission Monitoring

A basic and widely accepted definition of acoustic emission (AE) monitoring is the detection of transient mechanical waves in a source material. These waves are usually formed when a sudden change in strain takes place in a localized point by any of several possible methods. This means that when a crack or other flaw in a material creates some change in the overall material, usually through growth, there are waves formed that can be recorded and analyzed, as shown in Figure 2.1.

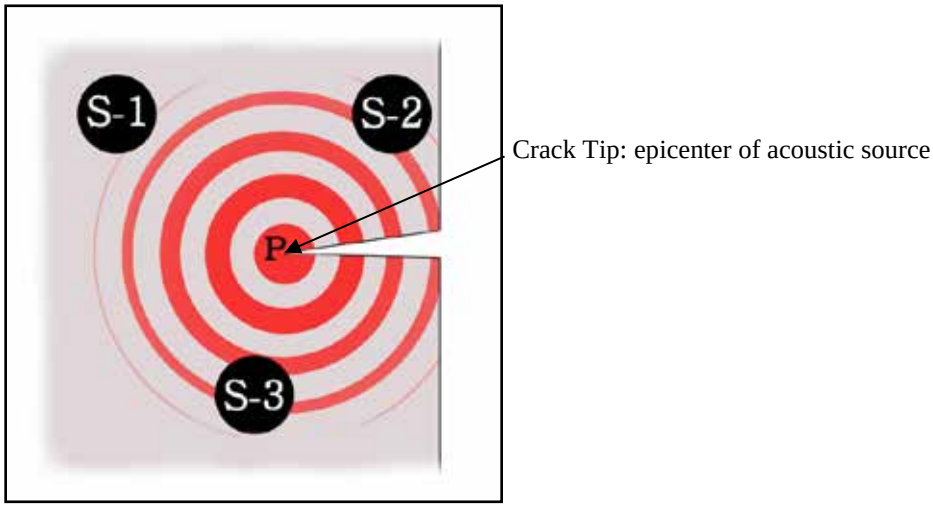

Figure 2.1: Acoustic Wave Propagation from Failure Point, P, to Three Sensor Locations: S-1, S-2, and S-3

Based upon this same figure it can be seen that the locations of the sensors are important, as the closer the failure epicenter, Point P, is to the monitoring device, the stronger the signal is. This gives the user an ability to locate the point of failure to some degree by use of triangulation methods.

A natural example of how modern AE works is by examining the propagation of an earthquake. In and around a fault line, forces and stresses are being built up over time. At some point the tension becomes too much and there is a sudden shift of the ground structure, whether on the surface or subterranean does not matter. When this event happens the released energy is distributed in sudden waves propagating out from the epicenter, resulting in large tremors. These waves are then used to determine the strength, location, and the type of event that created the quake. This is the basic principle to AE monitoring; it simply happens on a smaller scale.

2.1.1 Origin of Acoustic Emission Monitoring

The use of the AE monitoring method has been around for over half a century, but it hasn't been until the last few decades that it has truly expanded and come to be seen as a serious structural monitoring technique.

Acoustic emissions have been used for centuries by many civilizations in many parts of the world. Some of the earliest known examples are earthquakes, as mentioned earlier, and in mining practices. Workers in a mine shaft can often get some warning of an impending event by listening to or feel rumbling in a shaft. Often the sound can be heard before a cave in and is an alert that people should get out or take cover before a possible collapse occurs.

The first detected acoustic signals that were recorded for analysis occurred during a study by a Japanese timber miner named Kishinoue. In 1934, he developed a method of recording the acoustic emissions created during bending tests of quarter-sawn wood beams. "He transferred the vibrations (AEs) associated with the fractures of a board into an electronic gramophone through a needle on the board." The vibrating needle would create marks on cinematographic film that could be further inspected for AE events that took place during the bending tests (Kawamoto & Williams, 2002). While this method was used to determine the strength of trees that had been cut

down, a quite different method of AE monitoring was being developed in Germany to record their growth.

A man by the name of Forster was also analyzing sounds coming from plants in Germany, but not for structural purposes. Instead he noticed sounds created while the plant was growing and wanted to record the AE for further study. In order to do this, he developed a system that would measure the small voltage changes created whenever resistance changed in his recording device due to the sound wave passing through a strain sensitive material. This method, while used long ago, is basically the same as the current one employed by most of the world's AE monitoring devices (Kawamoto & Williams, 2002).

Monitors today are a combination of many components that work together to record the desired data; however, the majority of these pieces can be condensed into two parts. The first is the acoustic sensor itself. Even though these devices are small, they are also very important to the device as a whole, as without them there would be no data. The sensors are actually a form of transducer and are attached directly to the material being analyzed. Transducers function by converting the mechanical waves in the material into an electrical signal by using a special material called a piezoelectric crystal, or sometimes simply a Piezo. This material has the ability to generate an electric voltage when a stress is applied, creating a natural way to record small changes in a material's surface stress easily. When an acoustic wave is created, the compressions and tensions created can be picked up by the sensor and in turn the crystal material inside, creating an electric signal that can be recorded by the Data Acquisition System (DAQ) for further analysis.

The second main part is the DAQ or computer processor. Due to sophisticated DAQs, modern AE monitors can be self-sustained upon activation if given a proper power source and the correct information to perform the desired tasks. Most systems can be set up to monitor and record the data until the user wants the data to be sent remotely to a predetermined computer or File Transfer Protocol (FTP) site for analysis. The DAQ is also responsible for applying any thresholds deemed necessary to the project or getting rid of unwanted noise.

The sensors can come in a variety of shapes and styles, which can be picked specifically for the analysis needed. One of the most common options available is the frequency range of the

desired sensor. The choice of sensor frequency comes with benefits and drawbacks regardless of which option is chosen for the project. This is due to the nature of the acoustic waves; a high frequency wave will be very sensitive to acoustic events but typically will not have a large sensor range, leaving the sensors abilities limited. In this project, a sensor was chosen with a low frequency due to the large size of the structure being monitored and the amount of devices being used. However, a drawback in using a low frequency sensor is the effect of environmental and background noise, creating more data that will need to be filtered out.

2.1.2 Benefits of Acoustic Emission Monitoring

The first and possibly most important benefit to using AE monitoring is that it is a non-destructive test (NDT) that can be performed on a variety of materials and geometries without needing to remove them from service or otherwise harm them. This, however, cannot be the only consideration; there are many other NDT methods available including the following:

- Electromagnetic Testing (ET)
- Radiographic Testing (RT)
- Ultrasonic testing (UT)

If we compare the methods above, they are all able to detect defects within a material; however, upon a further comparison of the techniques, only one stands out as being suitable for the needs of this project. The first option, Electromagnetic Testing (ET), is composed of several possible processes that involve creating an electric-magnetic field or current within an object. The results can be analyzed and used to determine if there is a defect within the material by examination of how the field of current travels through the volume under observation. This testing process is used heavily in piping and tube manufacturing as it is able to be used proficiently on metallic materials such as steels and some irons. Due to the need for an electric or magnetic field creation in the material, it is virtually impossible to use on FRP materials and not considered a possible technique.

The next method listed, Radiographic Testing (RT), uses short wavelength radiation by means of using high energy photons, or in some cases neutrons, to determine what is occurring in the material. Unlike ET, this form of testing is not dependent on the conductivity of the material,

and the signal can pass through most materials without much difficulty. The amount of the radiated beam that passes through a structure can be collected and analyzed to determine how much was stopped or reflected away. This data can then be used to determine where and what kinds of defects are occurring within the observed part. The process has two major drawbacks in its general use, however: design and safety. The design of RT apparatuses makes them either too large or too easy to damage when placed in an open environment. Another issue with the design is the general use, where a transmitter and receiver are needed on either side of the structure, or in our case on top and bottom of the panels. While this would be fine if no one ever wanted to use the bridge, this most likely will not occur and would therefore not be possible. The parts could be placed on either side of the panels with a decrease in the accuracy of the results, but the second problem, safety concerns, still persists. The use of this NDT method creates radiation that could potentially endanger pedestrians or the environment surrounding the bridge. Because of these unwanted risks, RT is not a practical method to evaluate the structure.

AE and Ultrasonic Testing (UT) are similar methods that both use sound waves in order to gather information about possible failures in the material. However, the ultrasonic method is an active system, while AE is passive, in that it creates a signal to travel through the material to find cracks and defects in a material. UT involves the use of a transducer that creates a high frequency sound wave that can be used to detect flaws by either reflection or attenuation methods. With the reflection technique, the wave passes through the material until striking a flaw or other change in the material structure and is then reflected back to the source. This method is similar to sonar in that it uses an echo-location technique, but is dissimilar in regard to the linearity of the device. As the transducer is moved across the surface of an object with a gel or oil couplant, the sound is focused in a linear direction, meaning that it only detects what features are directly in front of the transducer. The second attenuation method has a source and reception sensor that produces the sound wave and detects what parts of the wave passes through the material to the other side, respectively. This method creates another situation in which the monitoring is only occurring between two points on the structure, and does not monitor for the creation of failure points and does little to determine if or how fast they are growing.

The passive AE system does not send a wave to detect cracks; rather, it detects the crack's own sound waves. As the crack grows, it usually will make a noise that can be detected by the AE monitoring system which in turn can be used to determine where the source is, if it is growing, and how quickly. If used properly, this method can neglect unimportant defects while larger ones are constantly monitored regardless of direction from the sensors, increasing the abilities and range of options in how the analysis should be conducted.

The many benefits and abilities inherent in AE is why it has been chosen as the medium to monitor the FRP bridges here, as well as many other tests performed across the globe. As discussed, the emergence of AE technology has shown to be very useful as a way to monitor structures both alone and as a compliment to other more classical testing and analysis methods. Due to the wide applicability of its use, AE has been used in a variety of industries to perform numerous jobs. Some of the industries that have made developments in the use of AE are the petroleum, aerospace, nuclear, and transportation industries. Some of the uses of AE in research are related to determining the properties of various pressure vessels, dams, toxic waste reservoirs, and of course bridge structures.

2.2 Acoustic Emission Monitoring on Classic Bridge Structures

While AE monitoring devices have been employed on a wide variety of structures in many industries, one of the most significant in terms of this research is that of contemporary bridge structures. In the United States alone there have been many applications of this technology in a number of locations and climates where AE has been found to be an effective method.

The British Ministry of Defense performed what is considered the first true use of acoustic emission monitoring on a bridge in 1971, when two researchers named Pollock and Smith demonstrated that the data from the sensors, as well as from other collection devices, showed a correlation with several results from other testing methods. This first analysis was critical for the future use of AE monitoring, in that it showed that with enough work, the acoustic monitors could be used to determine what events are taking place in the bridge without the use of other testing procedures (Sison, Duke, Clemeña, & Lozev, 1996).

In the year after the initial project, several other groups in the United States performed their own tests and, while successful in determining a correlation as well, they found that a problem did exist in the amount of noise that is also recorded by the equipment. However, this problem would be identified in the following decade as being due to the vibrations caused by vehicular traffic and in some cases environmental activity (Sison, Duke, Clemeña, & Lozev, 1996).

In the 1970s, FHWA made another development in the evolution of the long-term monitoring system. It was during this time that the first battery powered devices were designed and tested, resulting in the ability to place the systems in locations previously unobtainable due to power availability constraints. A self-supported memory system was also initiated, increasing the data recording possibilities. Now the system could both be placed anywhere and have a possibly longer recording time before the need for a user to get the memory from the system for analysis (Sison, Duke, Clemeña, & Lozev, 1996).

Soon after these leaps were made in the collection of the data, a renewed interest occurred in the 1980s in the direct meaning of the data. A variety of researchers looked at the various aspects of the AE results and the bridges the data were gathered from. The various projects included the identification of various types of events from the data recorded, the effects of traffic on the signal and the noise created, and the effects of the bridge materials on the overall acoustic signal. From these projects, a series of thresholds could be applied that would help alleviate the noise effects and record only the desired noise related to “unnatural” events (Sison, Duke, Clemeña, & Lozev, 1996).

While in use, a bridge is subject to a variety of sounds from traffic, pedestrians, the environment, and general background noise. In order to evaluate the ability of AE to properly monitor a steel bridge, Transportation Technology Center, Inc., performed a test to monitor cracks and crack growth in steel bridges. The results showed that background noise was able to be ignored successfully; crack commencement and growth of the cracks were still able to be detected by examining the hit rate (Uppal, Stone, & Kristan, 2000).

Since its inception in the 1970s, AE monitoring has developed into a reliable and heavily used monitoring tool on both small rural bridges and large highway bridges, including giant

suspension bridges. Departments of Transportation (DOTs) in both Wisconsin (WisDOT) and California (Caltrans) have used this technique on multiple highway bridges and successfully located possible failure locations during their application (Prine, 1995).

The Texas Department of Transportation (TxDOT) applies AE sensors to many of its bridges, including the Fred Hartman Bridge, shown in Figure 2.2. The bridge was officially opened in 1995, and is responsible for carrying State Highway 146 over the Houston Ship Channel. However, it was soon discovered that large oscillations occur on the stay-cables, and through visual inspection it was determined that the cables were creating cracks in the welds between the fixture holding the cables and the rest of the superstructure. In order to monitor the situation, it was decided that a fatigue examination of an AE device with four sensors, supplemented by strain gauge monitoring, would be conducted at the Ferguson Lab at the University of Texas on a similar cable specimen (Kowalik, n.d.).

Figure 2.2: Fred Hartman Bridge
Source: Bayareahouston.com (n.d.)

During the study, it was determined that there were several breaks at the anchor and near the loading end. In all cases the breaks were found within the section of cable expected or in a section next to it. Since 2002, the Fred Hartman Bridge has had three acoustic sensors on each of the 192 cables monitoring at a near constant rate. The data is also filtered in the main Data Acquisition System in order to expel background noises and send the information to a central processing unit where it can be categorized and uploaded to an online resource to be downloaded when needed (Kowalik, n.d.).

2.3 Acoustic Emission Monitoring in Fiber-Reinforced Panels

Acoustic emission (AE) monitoring has been studied in a variety of ways in conjunction to its possible use on composite materials, and as FRP seems to have branched off of the field of composites, many studies from each area can be applied to one another.

AE monitoring on composites has been around for over 2 decades and is constantly being developed by scientists and researchers for practical use in a variety of fields. Research has been heavily sponsored by NASA to study the use of AE on composite materials in various environments and conditions. Due to this sponsorship, it was determined that the extreme cold and conditions of space would most likely not be detrimental to the AE sensors as initially suspected by some, and they were able to perform their duty accurately upon reaching a temperature equilibrium with their environments (Walker & Workman, 1998). This and other projects have shown that AE monitoring has the ability to monitor composites reliably even in harsh environments.

As mentioned earlier, Piezo sensors are used in many AE devices, and therefore are an integral part of the structural health monitoring system. One of the last problems gripping the field of AE sensor use is the bonding ability between the AE sensor and the structure, and its bond stability. To make this connection more effective, studies are being carried out for the Air Force Office of Scientific Research at Stanford University using yet another material common to composites, carbon. If used properly, carbon nanotubes should reinforce the bonding structure while creating a more reliable path for the acoustic wave to travel to the sensor for recording. While further testing is needed, the work in this area looks to improve the reliability of not only the sensor's bond, but the sensor's ability to record data overall as well (Lanzara, Zhang, & Chang, n.d.).

However, being able to receive and record data and analyzing data are two different things. If the data received is unable to be understood, or does not mean anything to the researcher, there is no point in the monitoring in the first place. Luckily, the AE technique has been studied in its use on composite panels for some time and is understood enough to determine if there is a problem and possibly where it is located.

To help understand the acoustic relationships in experiments, a cut was applied to the specimen so the failure source location could be better controlled. The results showed that failures cause both high and low amplitude emissions; it depends on the type of failure, longitudinal splitting, and fiber fracture. In the tests performed by Ely and Hill (1995), the analysis determined that the amplitude data could be divided into two bands divided at 60 dB. While subject to interpretation, the possibility that two failure types produced noticeably different data in terms of amplitude was an interesting development.

Indeed, it appears that the lower amplitude and energy sources were closely linked to the longitudinal splitting, while the higher valued ones came from the fiber breaking. This is further supported by the lack of event buildup before the longitudinal failures, while it was certainly present before the fiber failure. This would be expected as in many tensile tests, sounds can be heard simply by the human ear moments before fiber breaks, but usually not as much before matrix failure. Another reason that gives support to this is that upon thinking about it, one would expect a fiber break to result in higher energy events due to the larger stress build-up that has occurred in relation to a matrix material.

Chapter 3: Experimental Method & Analysis

Development of a monitoring system for fiber-reinforced polymer (FRP) bridge panels is the central focus of this research. Earlier projects performed at Kansas State University examined the thermal effects on an FRP bridge located outside Russell, Kansas, in addition to developing a possible repair technique for panels that did experience failure. These findings led to the need of a method that can accurately determine the deterioration of the bridge by various methods, including fiber breakage and delamination.

3.1 Project Stage Background

The overall acoustic emission project has consisted thus far of two stages conducted by individuals at both the University of Kansas and Kansas State University (Gostautas, Ramirez, Peterman, & Meggers, 2005). The first stage was performed by Richard Gostautas of the University of Kansas and consisted of determining if acoustic sensors would be capable of detecting the failures experienced by the panels in controlled tests. Another element examined was how the acoustic emissions change with the application and removal of loads.

To do this, a set of five sensors were attached to a series of panels, widths varying between 6 and 30 inches, during bending tests that included failure examinations. Two sensors were attached to the top, two on the sides, and one on the bottom during each testing session. The tests consisted of an application and partial removal of load at the center of the beam by use of an I-beam oriented perpendicular to the panel length. The early examinations had to do in part with determining the Felicity Ratio, the value corresponding to the Kaiser Effect in the FRP panels. The Kaiser Effect is a trend related to acoustic emission, where the acoustics are recorded during load application and partial removal. When the force is reapplied, the acoustic readings do not initially commence. The emissions do not occur until a particular stress is obtained at some fraction of the originally applied load's maximum value. A general graph of the loading cycle used during this analysis is shown in Figure 3.1.

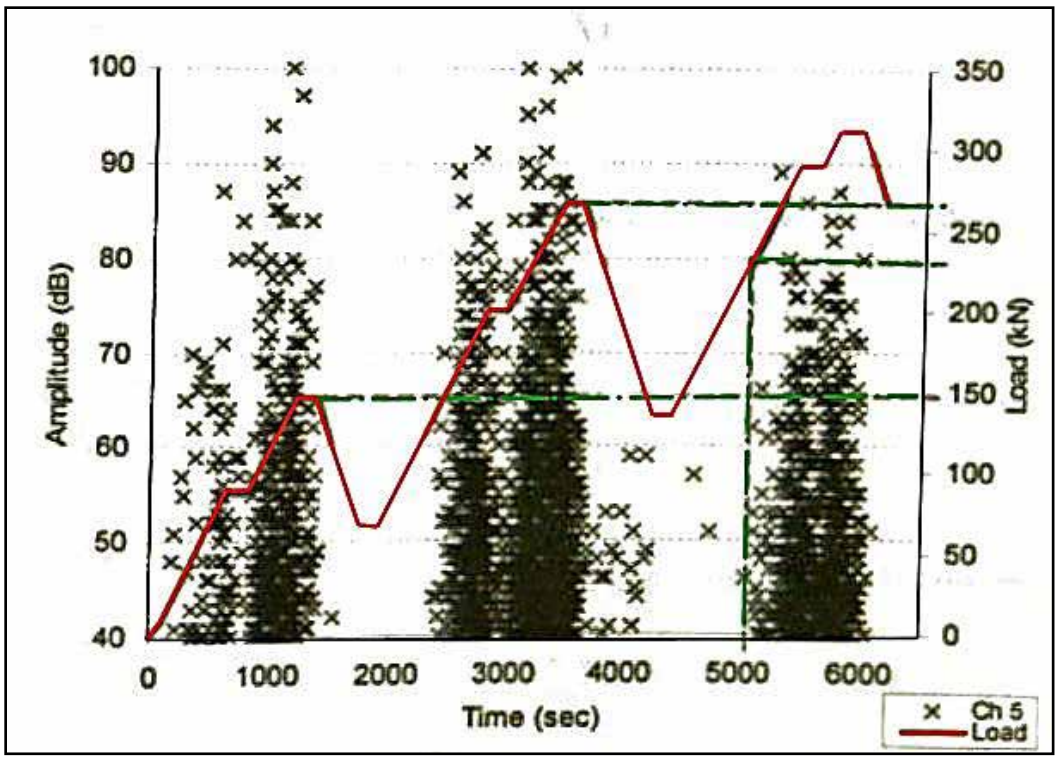

Figure 3.1: Load Application in Keiser Effect Analysis
Source: Gostautas et al. (2005)

From examining the Keiser Effect, it was demonstrated that the emissions recorded occurred when the loads were being increased and occurred more often after the previous maximum loading peak was approached. This outcome would be expected, as an increase in the load would infer an increase in the stress of the panel, as well as the fibers and matrix within it. In order for the material to remain unbroken, it would have to be able to support a stress equal to that experienced in earlier peaks, and would therefore not fracture until a higher load was applied.

The second analysis performed has to do with the ability to determine what properties are related to and occur during a panel's failure. Gostautas concluded that a graph of zones could be used to aide in the classification of the type of failure being seen during the analyses, but several of these areas overlap making it difficult to classify all failures into a specific type. A general layout of the Amplitude-Duration Zone chart is shown in Figure 3.2.

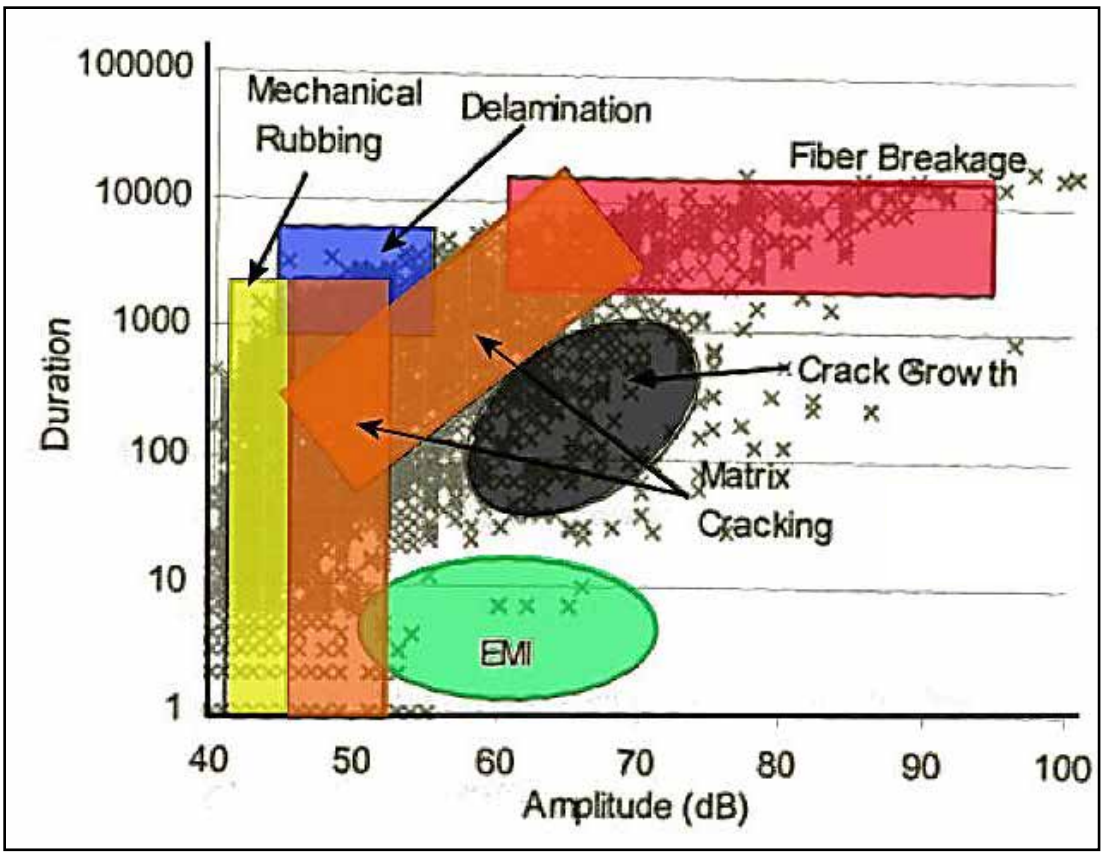

Figure 3.2: Cross Plot of Duration versus Amplitude
Source: Gostautas et al. (2005)

One of the last areas examined had to do with the repairing of FRP panels and retesting the structure. Upon failure, the panels would be repaired by placing an outer wrapping on the structure and retesting it to determine if the structure is reusable. The determination was that the previously failed and repaired specimens were able to carry a larger load without failure while creating more acoustic noise. This stage of analysis determined the acoustic tendencies of the overall structure and examined how, by use of a linear technique, a failure location might be determined when between two sensors.

In the second stage, discussed in this paper, the analysis will be on the use of a network of acoustic emission sensors to determine the failure type and location. In addition, this research looks at the transfer of an AE wave between two panels, further analysis of noise distribution, and initial design set-up for a long-term monitoring system is performed.

3.2 Equipment and Software

3.2.1 Equipment

Hardware able to handle multiple devices and apply a variety of user defined constraints, while maintaining a quick rate of data collection from the sensors, is the central method being used for the sensor network analysis. The Sensor Highway II Data Collector (SH-II DC) was built by Physical Acoustics Corporation (PAC) and designed specifically for the current and future needs of the overarching project. It was designed to provide the most functionality while maintaining an easy operational setup and having the ability to work for a variety of setups.

The SH-II DC system is a data acquisition module comprised of many individual components. The overall DC is located within its own enclosure, protecting it from the environment and allowing all the parts to be in a controlled, safe space regardless of local weather conditions. The complete enclosed system and the Dell Laptop PC used to communicate with the system in this project can be seen in Figure 3.3.

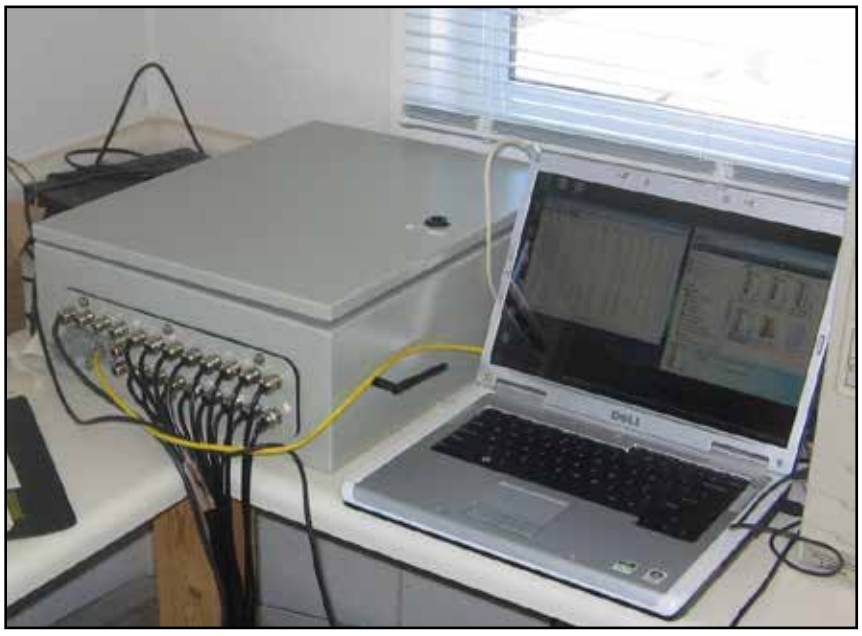

Figure 3.3: System Enclosure and Laptop PC at Testing Site

The system includes four 4-channel signal-processing modules, allowing data from up to 16 sensors or other measuring devices to be monitored, processed, and saved concurrently. The

data received from these modules is stored on a CompactFlash memory card capable of being removed to get the data directly if the need arises or is desired. The system is powered by an external source of either AC or DC power which enters the system through a surge protector and is in turn connected to the Circuit Breaker, allowing direct control of the entire system's power and an additional line of protection from electric surges.

Various connection ports are located on the system for different types of communication with the exterior devices. Other than the power input, network, or PC connections, the sensor wires can also pass through the enclosure while maintaining a total seal and connect to the inputs on the 4-Channel boards. On the right side of the enclosure, partially seen in Figure 3.3, a port allows the system access to a communication antenna connected to a PC modem found within the case. It is through this device that remote connections can be made if alterations are needed while the user is off site, and more importantly the data can be sent from the on-site location to an FTP website that can be accessed separately through a standard network connection.

The AE sensors recommended and supplied with the system are described as piezoelectric transducers, which are known for being highly sensitive to acoustic waves while remaining relatively cheap to create and maintain. In order to make sure that the acoustic waves are able to pass from the object to the sensor, there must be a suitable substance between the sensor and the structure to maximize surface contact and wave transfer. This is usually done by use of an epoxy adhesive or grease on the material and sensor while being held in place with clamps. However, due to the size and shape of the structure in this project, clamping would prove to be difficult, and an epoxy adhesive may damage the sensors when it comes time to relocate them on the structure. For these reasons, a silicone caulking was used to create a firm connection between surfaces. This material is also able to be removed rather easily when it is time to move the sensors themselves, without any recorded damage to the devices.

3.2.2 Software

The software designed by PAC is able to perform a variety of operations in both live-action and post-processor conditions. However, the first step in setting up the unit's software is the same in both cases. In order to properly use the system, the software needs to be configured

to how the user wants it to function and what the parameters are needed in its use. This can be done simply by accessing the CF memory card from the system by connecting it directly to a personal computer. Eventually, the final part of the overall project will have the system use a wireless modem and connect to an FTP site at Kansas State University, but for the laboratory analyses being performed, the system was configured to allow the laptop computer to communicate with the system through Ethernet ports.

In order to accomplish this, the system was configured to work on a local area network (LAN) and be given a static IP address. After initial setup, the card was able to be accessed through Ethernet cable and the use of an FTP connection. At this point, the system was ready to communicate with a separate PC by Ethernet connection or simply save all incoming sensor readings to the storage card for future use.

3.2.2.1 Communicating with the System

The first piece of programming is called “SH-II Client,” which has been created by PAC specifically to communicate with the SH-II system after a hard-line, dial-up, or wireless connection has been established. After the installation is complete, there are multiple ways to make a connection; in this experiment the best way would be to use an Ethernet cable due to the proximity of the computer and system.

From here thresholds can be applied to all the sensors so that if there is a hit that occurs outside this filter, it can be ignored immediately and not subjected to being analyzed on a sensor by sensor basis, thus saving time. Another ability of this program is a real-time Line Display of the sensors’ recognized and recorded events. In the future stages of the project, configuration of the system to upload files to an FTP site for data collection will be used in order to further utilize the remote capabilities.

3.2.2.2 Accessing and Using the Data

The data being stored on the flash card can be accessed by either direct or remote methods. Direct is the easiest to perform, where the memory card is removed from the system and inserted into a card reader for access. The remote access options allow the memory to be

acquired by the user without stopping the system from collecting data. For the current stage of the project, the information can be collected using a remote method. The user connects to the system by use of an Ethernet cable and opening an FTP site window. Using an IP address and administrator password setup earlier for the system, the flash card can be accessed directly.

Upon collection of these files, the AEwin for Sensor Highway E1.00 program, also designed by PAC, is used to manipulate the data into a usable form in any of several user-designed graphs. The primary functions of this program are to replay the data as if it was being collected live, creating useful charts in both 2D and 3D formats, combining separate files, and converting the system's DAT file into a text file, allowing it to be uploaded and used in spreadsheet programs like Excel. This was used extensively to compare the initial data to the loads being applied to the structure at the time. With this option, the load applied and resulting acoustic data being recorded can be examined quite easily with or without filters being applied to the file if needed.

3.2.3 FRP Construction and Test Setup

Three FRP bridge deck panels were built by Kansas Structural Composites, Inc., designated Panel-A, Panel-B, and Panel-C for the purposes of this report. Each is comprised of a mostly hollow 74-inch-long × 102-inch-wide × 6-inch-deep structure made of glass fiber-epoxy material designed by the Kansas Structural Composites after stage one activities were completed. This design consists of three layers of plates laid up to create a sinusoidal wave and stacked upon one another with a flat layer of fiber between them. The structure was then wrapped in chopped-strand mat and the epoxy resin was allowed to harden; the resulting plates have a ridged cross section but are capable of tolerating applied bending forces. Throughout the tests discussed, Panel-A was monitored at all times to some degree, while Panel-B was monitored only during instances in which interaction between two panels was being observed. Panel-C was not used in this research at all and was held in reserve in case massive failure occurred in Panel-A or Panel-B or as a reaction panel for constraint to the other panels. Panel-A can be seen in Figure 3.4.

Figure 3.4: Panel-A on Testing Platform

The overall structure of the panels was designed to allow bending forces to exist without damaging it to failure under regular loading cycles. To help create added strength to the bridge structure, when used in series the decks will be interlocked with one another by use of tongue-and-groove connections on either end of the structure as shown in Figure 3.5.

Figure 3.5: Close-Up of Lip-and-Groove Connection Between Two Panels

During the analysis phase of this project, each panel is supported on four steel I-beams spaced with regards to the ends of the panels, with one located at roughly 4 inches and 28 inches from either end. For a better understanding, a depiction of this can be seen in Figure 3.6. These beams are held in an elevated position by each end, allowing vertical movement of the structure and the bending from applied forces to occur.

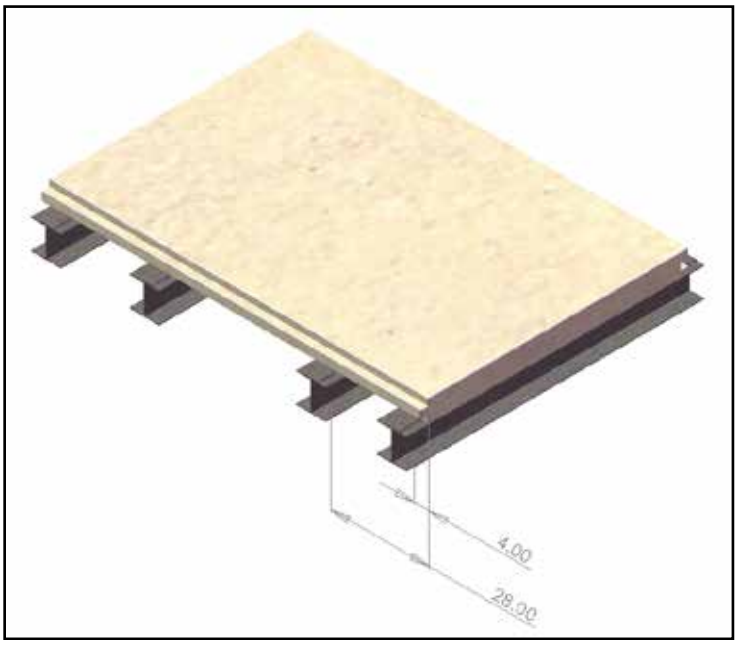

Figure 3.6: Bridge Deck and Support Beam Relation

The bending force is generated by a pneumatic cylinder statically suspended over the structure, capable of applying forces anywhere on top of the panels. These forces can be in excess of 35 kips and applied in a way that allows for distribution to be over an area approximately the size of an automobile tire. This distribution is achieved by use of a distribution pad on the end of the piston, consisting of a steel plate and rubber-foam matting. This setup is similar to the one used in earlier analyses, except the forces exerted in this analysis are less than half of those used in the first stage. This is in part due to the analysis not requiring failure to occur, but just to examine how the data and sensors can be used to determine a source location. In addition, the first stage used a method that created uniform bending, where this stage uses a more specific loading location, allowing for the acoustic data source to be approximated easily;

the most likely source will come from the point at which the plate is being exerted onto the panel, giving more accurate results if the plate is smaller. The items used to produce the direct force can be seen in Figure 3.7.

Figure 3.7: Pneumatic Cylinder and Distribution Pad

For the tests in this project, the same procedure was applied in each case with the only physical changes being where the application of the force would be and the layout of the AE sensors. These changes in sensor location occur in response to the acoustic property being examined at the time as well as where the applied force is in the series of tests. The force location will be carried out at predetermined locations corresponding to placements between or over the beam supports under the panels.

During this stage, there was also another set of analyses conducted by Dave Meggers, who hopes to determine how the beam deflection, stresses, and strains are related to each other

by use of the data from the pneumatic cylinder, linear deflection, and strain gauges. Some of these strain gauges can be seen in Figure 3.7, in the bottom left corner.

3.2.4 Thresholds

One concern of using this monitoring method is that the amount of data collected could create files so large they would become a problem when it is time to transfer them over the modem. In order to decrease the file sizes, the data was analyzed with a variety of thresholds being applied to remove background and noise readings.

Before moving into the discussion, it should be mentioned that energy, absolute energy, and signal strength are all measured in 'Counts' which correlate to usable values. According to Physical Acoustics, each energy and absolute energy count is equal to $10x10^{-6}$ V-s, and a strength count is approximately $3.05x10^{-12}$ V-s. Since the use of these values in this stage is purely in comparison to others of the same property, and conversions or equations will not be heavily used, the values will remain in counts for the remainder of this project.

Initial tests were conducted to determine if the system worked and what thresholds could be applied to the system during this analysis to remove as much excess noise as possible and focus on useful data. When no threshold is applied, the background noise consists of persistent sounds that come from environmental sources, such as wind, rain, and animals. While many other sources exist, two of the largest in this project are traffic and machinery noise. In this stage, the traffic noise cannot be simulated to any reasonable degree, therefore the focus will be placed more on any constant noise that occurs during the tests overall.

The two properties considered for thresholds are those of amplitude and energy. In the setup a hit is recorded each time a rise in a signal's amplitude is high enough to be detected by the sensors. The peak of this signal rise is most often recorded as the hit's amplitude, and the amount of time that the signal is recorded before dissipating is referred to as the signal duration. This is what was used for the graph in the earlier stage to identify the types of failure being recorded. The energy is a value of the work output created by the transverse waves as the signal passes the sensor location.

The initial test was performed by placing the sensors on Panel-A in a set of two arrays with two sensors located at points of interest. Array 1 consisted of sensors S2, S5, S8, S11, S13, and S16. Array 2 consisted of sensors S3, S4, S5, S7, S10, S12, and S15. Due to the damage on the corner sensor, S1 was placed on the side of the panel 4 inches from the corner. The other separate sensor, S9, was placed 2 inches from the joint edge and 71 inches in the X-direction, as shown in Figure 3.8.

The sensors in the Array 1 were located in the X-direction beginning at 1 inch at 20 inch increments with the last sensor at 101 inches, and 18 inches from the joint edge. Sensors in Array 2 were placed 28 inches from the joint edge, with the exception of sensor S10, located at 24 inches. Sensors in Array 2 were located in the X direction beginning at 1 inch with a variable spacing ending at 101 inches (Figure 3.8). The force was applied between the first and second beams at 10 inches from the joint edge. This arrangement placed the closest sensor to the load at approximately 9 inches, with the next closest at 18 inches.

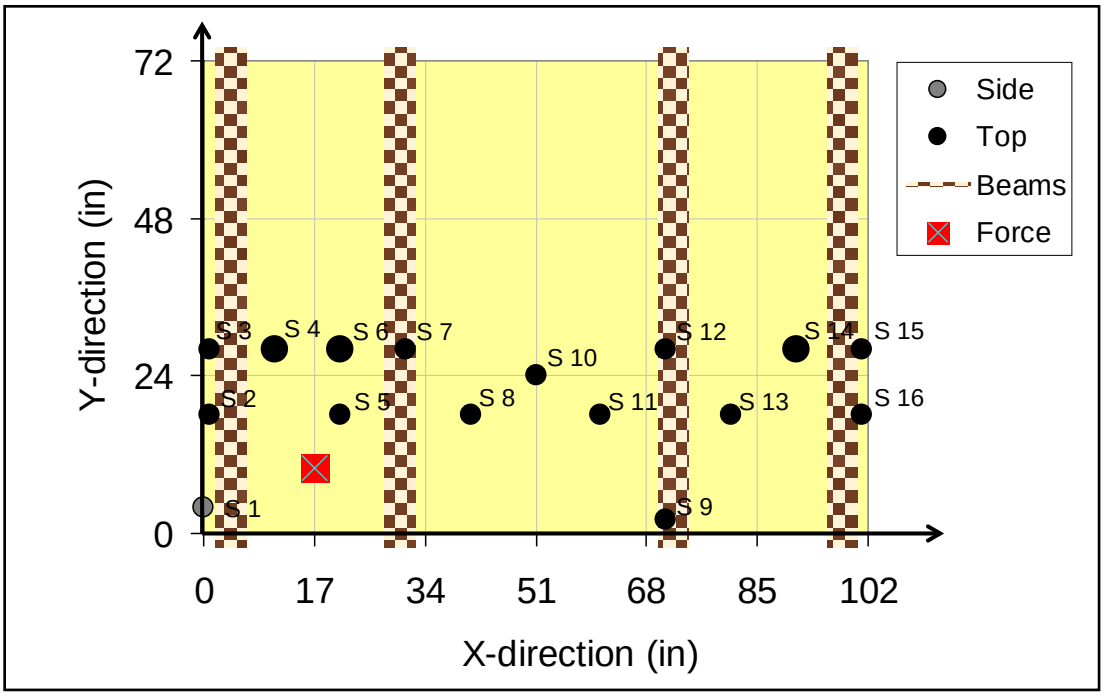

Figure 3.8: Threshold Sensor Arrangement

During the test, the load was applied twice to the panel; recorded acoustic data for both tests and the loading profile can be seen in Figure 3.9. The information gathered during the second application shows that there was a nearly-constant amplitude reading at about 35 dB, indicating a possible environmental or mechanical noise being detected. When left to record data while no load was being applied, the system reported hits were nearly constantly occurring between 20 and 40 dB. During subsequent testing, a threshold of at least 35 dB would be applied to the system, and in later laboratory tests the threshold would be increased to 48 dB, to both remove noise and aid in keeping the file sizes small enough to be transferred easily.

A comparison of the data before and after the filter application can be seen in Figure 3.10. The use of this single filter had a large effect on the file size as well as the data plots. The original data file was 32 MB for a test lasting just under 1.5 hours. With the filter applied, the data file was reduced to only 2.42 MB, roughly 8.5% of the original file size. Also the characteristics of the data changes during increased loading occurrences were still present after application of the filter.

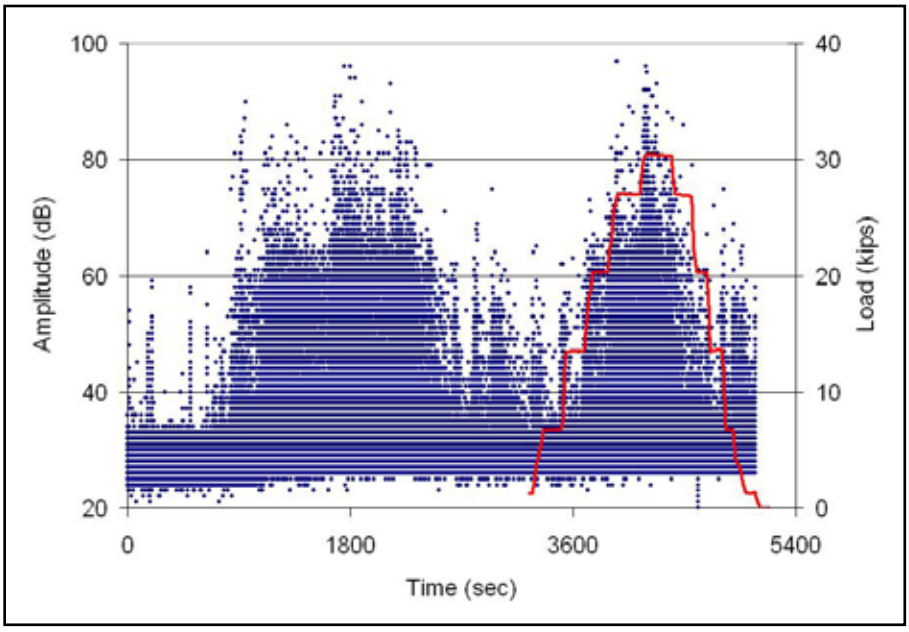

Figure 3.9: Initial Analysis on an Amplitude versus Time Scale

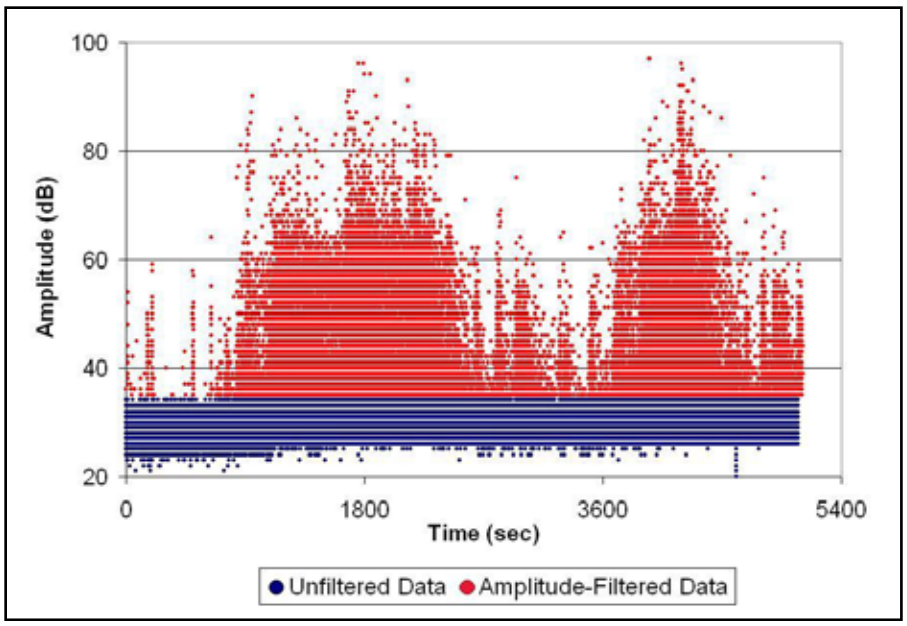

Figure 3.10: 35 Decibel Amplitude Filter Comparison

The next property that was evaluated was the energy of the hits. These values can be seen in Figure 3.11 as blue and green dots. There seems to be a pattern of dots forming at about every 10 counts, and several clusters at the 90 and 100 counts mark. If a 60-count threshold is applied to the data already setup with the amplitude threshold, the green dots in the figure are the remaining points.

With this new threshold, the data file actually decreases another 13.6% to 2.09 MB, thus increasing data transfer even more. At this time the original unfiltered data was revisited and had only the 60-Energy Filter applied, with a resulting file size of 23.5 MB. This is a 26.5% decrease in size, and while not as great as the decrease from the amplitude filter, it is still significant.

In Figure 3.12, a comparison of the amplitude charts before and after the energy threshold is applied can be seen, and indicates that it had minor impacts on its appearance.

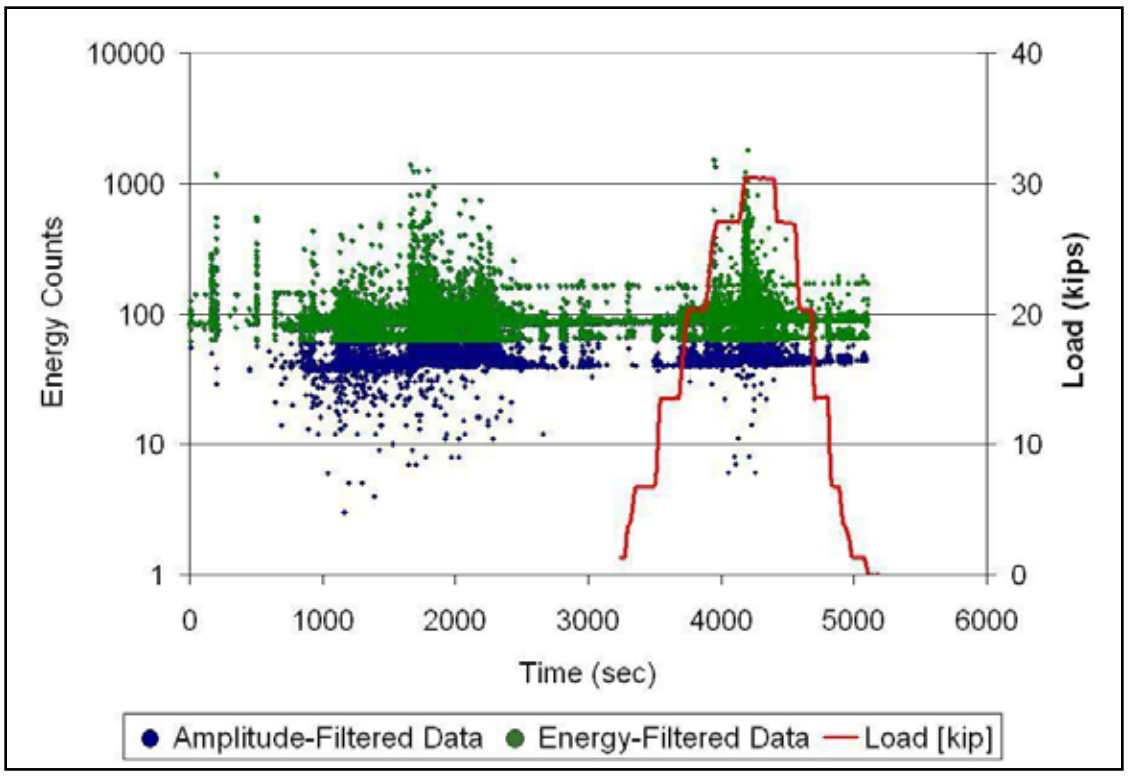

Figure 3.11: Energy Comparison of 35 dB Amplitude and 60 Energy Count Filter

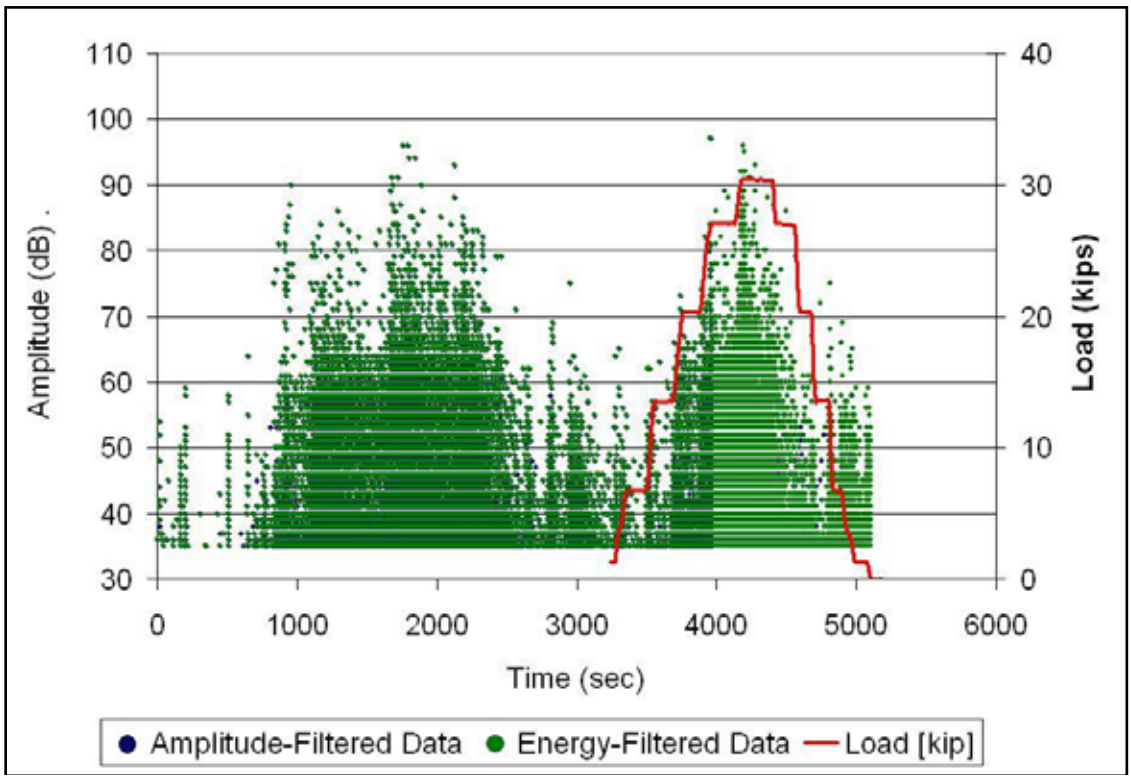

Figure 3.12: Amplitude Comparison of 35 dB Amplitude and 60 Energy Count Filter

If the filter level is changed to 80 energy counts, the chart is not significantly altered from the previous, but if an 85-count threshold is applied, the chart starts to show significant change, as can be seen in Figure 3.13 where hits at the initialization of the analysis seem to disappear. This is most likely a result of some sort of settling occurring in the panel, or small fractures forming and expanding during the first loading cycle and breaking more in the second.

A hit occurrence chart can be seen in Figure 3.14. There are a large number of points located below the 35 dB mark on the chart, appearing between 10 and 100 times more often than the rest of the hit values. By applying the 60-Energy Filter the data decrease appears to be on the lower end of the remaining amplitude data points. There seems to be a small hump of data between the 35 and 48 dB values remaining, and a majority of the second filter takes the data out of that section only.

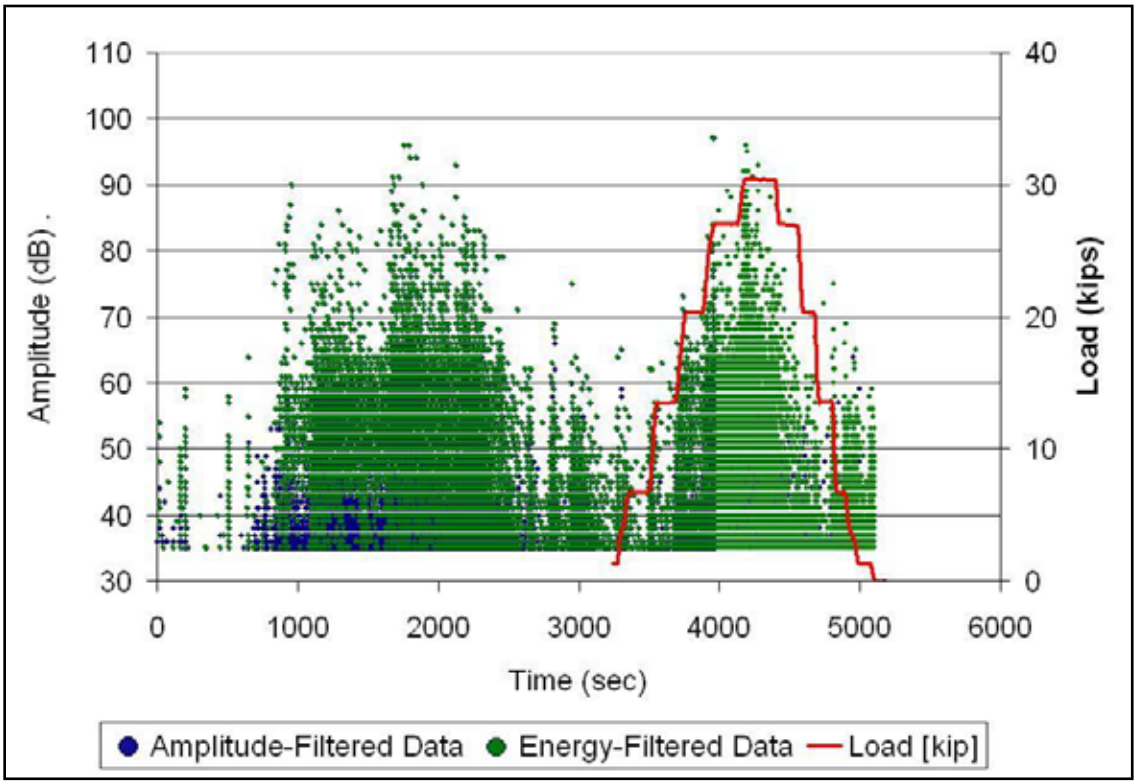

Figure 3.13: Amplitude Comparison of 35 dB Amplitude and 85-Energy Count Filter

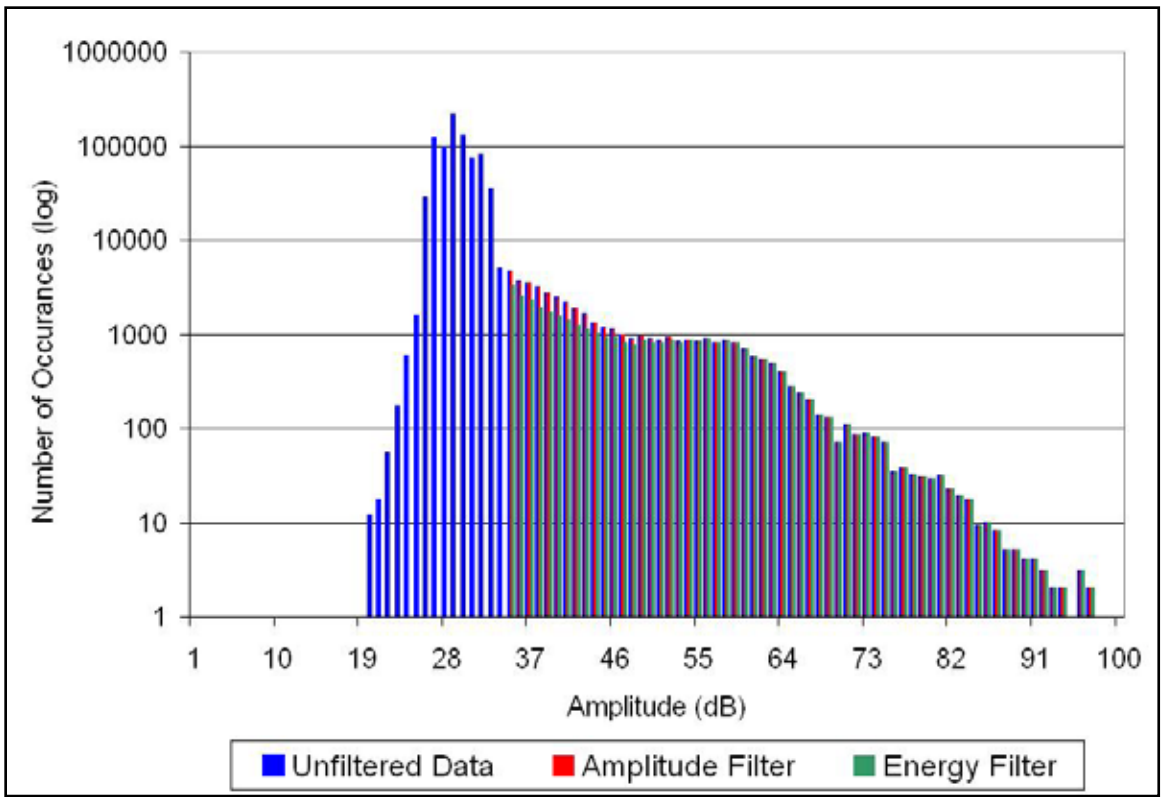

Figure 3.14: Change in Hit Number by Applying 35-Amplitude and 60-Energy Filters

During this stage of testing the file size is not important, as the data will not be transferred remotely, and therefore the thresholds used at this time will include an amplitude filter, as well as filters for values below 1,000 for signal strength and 100 for Absolute Energy. The data is not limited as much as the filters presented for possible future use, but does remove data at lower Energy Counts.

3.3 Signal Distribution in Single FRP Panels

The future bridge sensor layout will need to be built so that the limitation of a sensor does not become a limitation for the entire sensor network. To do this a series of tests were conducted to determine what manageable range the sensors have and how features in the panel affect the signal's ability to be recorded.

3.3.1 Basic Analysis of Single Panel Load Response

There were two tests completed over each of the first three beams, as well as one between the two interior beams. The tests themselves consisted of an increasing step load being applied over time. The first load would start at 1,000 pounds and increase incrementally to the maximum load being targeted. The increases in load would occur over a few seconds, the load would be held for at least 2 minutes, and then the next load increase would occur. Upon reaching the maximum desired load, it would decrease in a similar step fashion until reaching a load-free state.

Before continuing it should be noted that while the original intent was to take the load to a maximum value of around 22.5 kips, there was a calibration error in the load cell used by the facility performing the load tests, and actual maximum loading was 30.8 kips. This was not discovered until after a majority of the tests were performed, and resulted in an increase in the load of about 37 percent. The analyses presented here have reflected the appropriate change in the load values, but as stated, it was not the intent to use that much load during the earlier stages of this project.

For the first evaluation, the data will be displayed as a function of time with the applied loads overlaid on the graph. From this we can determine if there is a relation between the AE values and an applied load. This is the first step in determining if AE monitoring can be used as an acceptable form of determining structural damage to the panel. While the panel is not actually experiencing overall failure, the increase in stress should cause small fiber and matrix breaks, as well as general mechanical noises.

This test will have all the sensors on Panel-A in the same configuration as was used in the initial threshold test as shown in Figure 3.8, in a set of two arrays with two sensors located at points of interest. The forces were applied at various locations on or between the support beams in the tests, but the following data comes from the force application between Beams 1 and 2 as was used for the threshold.

From Figure 3.15, we can see that there is indeed an increase in the AE activity whenever the load applied increases and response appears to be proportional. This means that when the

load increases, the amount of AE data created appears to increase in both the magnitude and amount of hits.

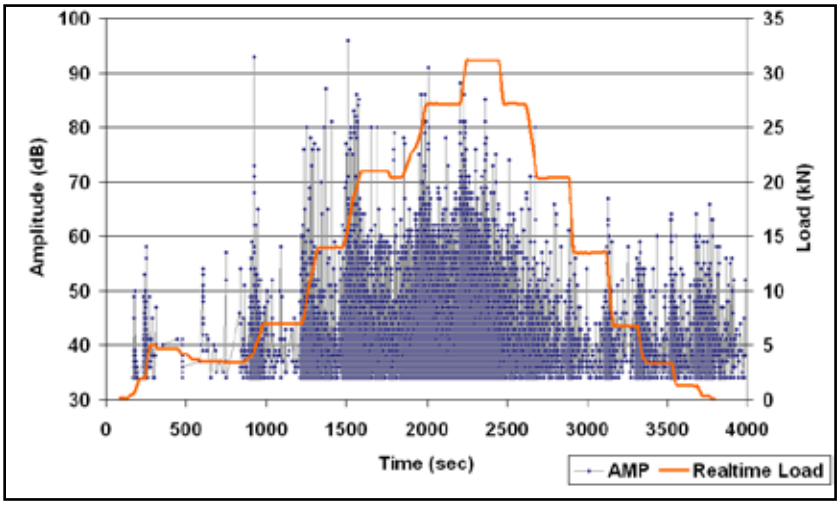

Figure 3.15: Initial Test, Amplitude with Force Overlay

It is also reasonable and shown in the figure that when a larger load is obtained, the AE activity occurs without a significant drop. This is most likely due to continuous fiber breakage and resin cracking; as the load is applied, the initial weaker fibers within the structure will break along with weak spots in the resin. This breaking of materials creates an increase in the amount of stress being experienced in the remaining local structure; these pieces then fail as their ultimate stress values are surpassed, creating more stress for the material, and the cycle continues. This scenario can also be seen in the values of energy and signal strength charts included in Figure 3.16 and Figure 3.17. These properties experience a greater amount of variation in their values, and need to be displayed on a logarithmic scale in order to get a greater understanding of the information.

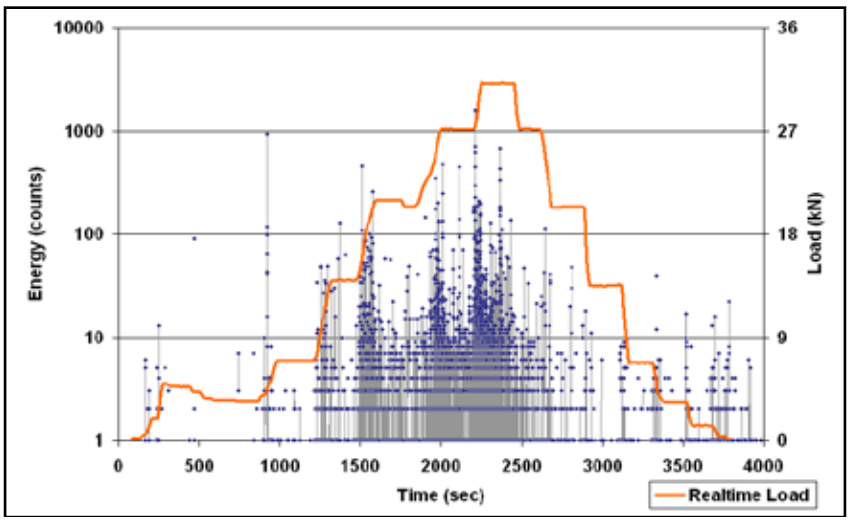

Figure 3.16: Energy Response with Load Overlay

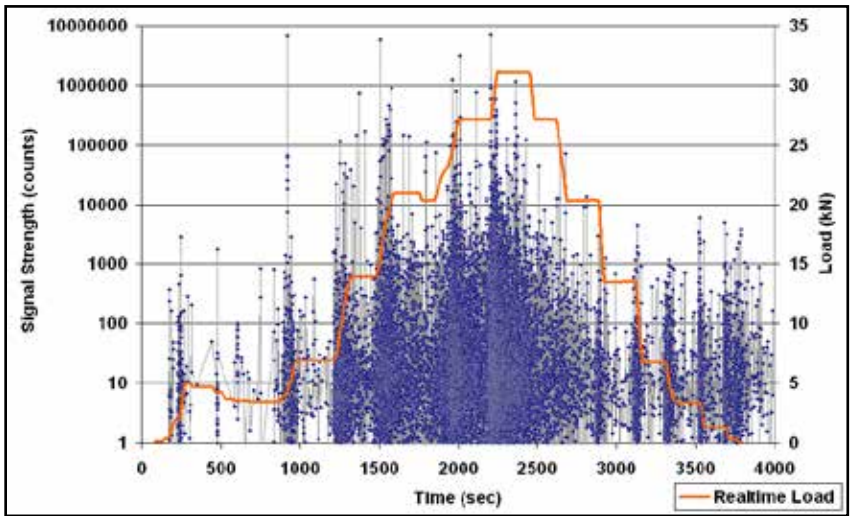

Figure 3.17: Signal Strength Response with Load Overlay

3.3.2 Single Panel Acoustic Dispersion Analysis

The sensors were arranged in two arrays along the top of Panel-A, as with the earlier tests, with sensors S4, S6, and S14 placed on the underside of the panel, as shown in Figure 3.18. By doing this, an accurate assessment of what the degradation of the acoustic properties is in relation to increasing distance from the source can be generated effectively.

As stated earlier, each test had a force applied on and between each beam; only the data from the load applied at the midpoint between Beam 1 and 2 will be discussed here.

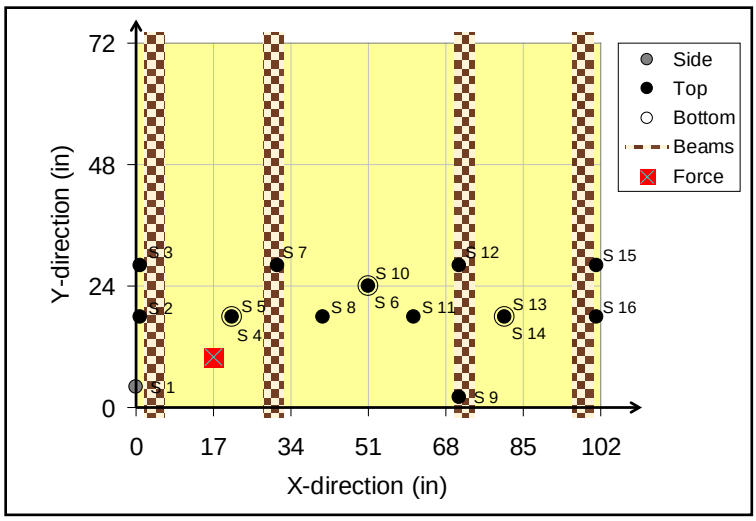

Figure 3.18: Signal Dispersion Sensor Arrangement

In this case, three tests were conducted in which the force was applied in the same location and in the same manner as in earlier tests by stepping up to a force of about 30 kips and stepping back down again. This will present the opportunity to see if the results of a test can be repeated and still get approximately the same data, or if there is any pattern to the results at all. After the tests were concluded, the results were graphed in terms of where the sensor was located horizontally with the panel's width. The force was not located in-between or on either line of sensors, but was located at 10 inches from the joint edge, placing it approximately 8 inches from the array made up of sensors S2, S5, S8, S11, S13, and S16. This set of sensors will be designated Array 1 to make it simpler to discuss in the rest of the paper; the second set will be designated Array 2. This set is made up of S3, S7, S10, S12, and S15. The S10 sensor was included in this array even though it is actually located between the two arrays to set a reference point between the S8 and S11 points in later graphs.

The first analysis was conducted to determine what effect the loading amount has on the properties of each sensor. In Figure 3.19, it can be seen in general that as the force value increases, the magnitude of the absolute energy also increases in each of the sensors. As would be expected, the sensors near the loading zone show an increased magnitude in relation to the other sensors, causing a peak response to occur around the sensor located at the 21-inch mark, S5.

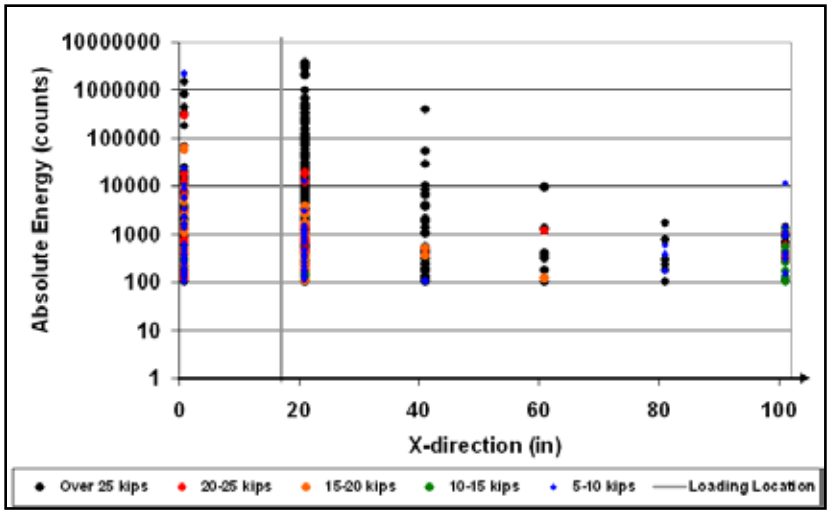

Figure 3.19: Absolute Energy Values Across Sensor Array 1

This occurrence was also found to happen in regards to the signal strength, amplitude, and the general number of hits. The values were found to focus on one section of the array quite well when tests were conducted above the 25 kips mark, which is most likely due to the high number of hits, as shown in Figure 3.20, that were detected during this period of heightened force application. If the values for loading over 25 kips are removed from the graph, response is still similar for the other four load ranges. Initially a large number of hits occur when the force is lower due to poorly bonded fibers breaking or ripping from the resin matrix or the panel settling on the bearings and aligning. Once the superficial failures have occurred, the response begins to increase with the increased loading as expected. From these multiple graphs, a definite pattern of increased activity and magnitudes can be seen near where the force is being applied which corresponds to the increase in loading as expected.

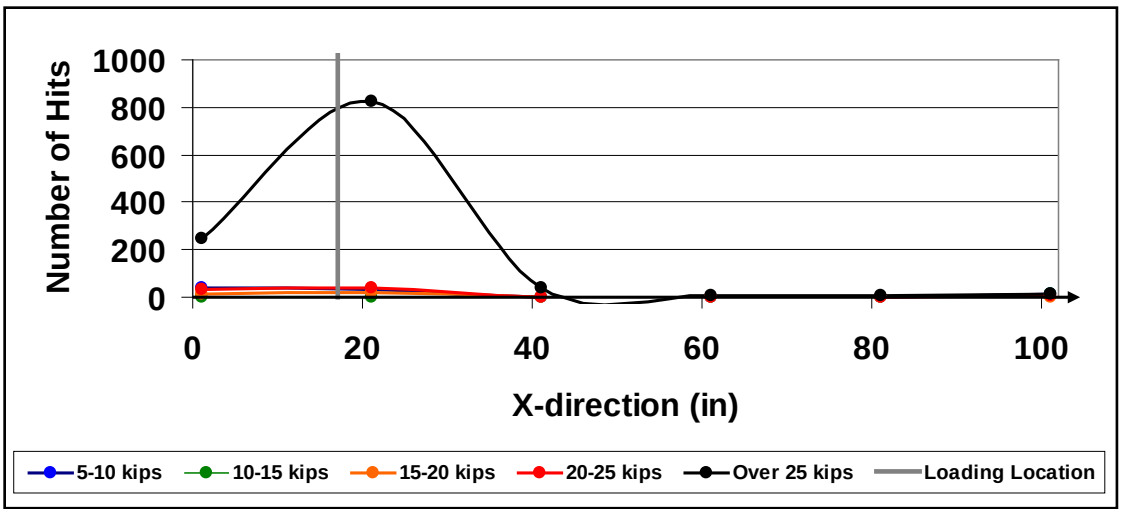

Figure 3.20: Number of Hits Across Sensor Array 1

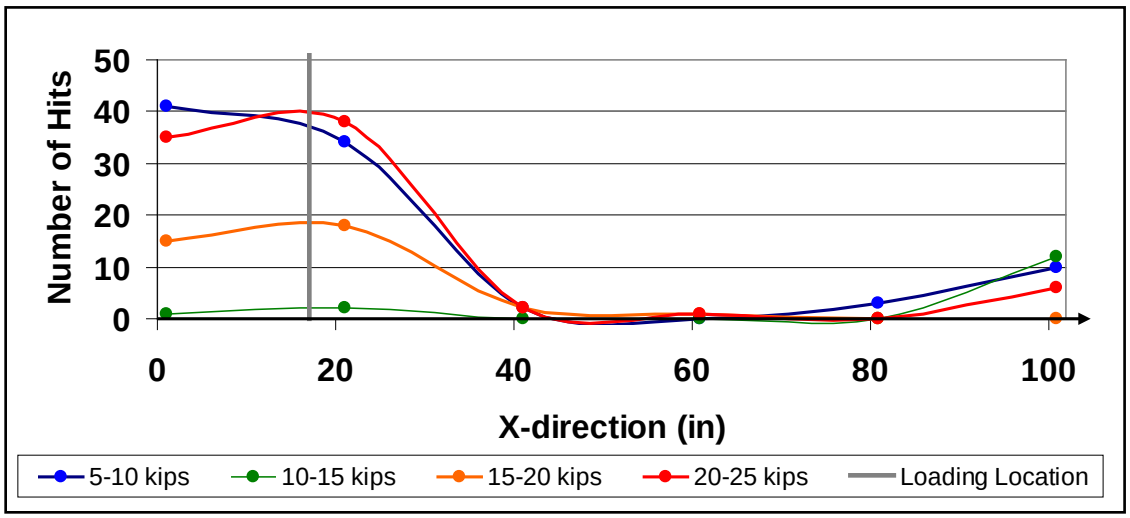

Figure 3.21: Number of Hits Across Sensor Array 1; Between 5 and 25 Kips

If the number of hits that each sensor detects is plotted, as in Figure 3.22 and Figure 3.23, the hits can be used to get an approximate location of the loading point. In terms of the testing order, the pattern of decreasing in magnitude in subsequent tests does occur once the load is over 25 kips, but there seems to be an inconsistency when the load is below 25 kips. However, the values are still similar in terms of the location of magnitude. The high number of hits for the third test could have been caused by rapid loading, shifting of the panel on the bearings, or the failure of a weak bond between the core and the structural skin. In either case, each test still

could be used to determine the general area where the source is located in respect to the array of sensors.

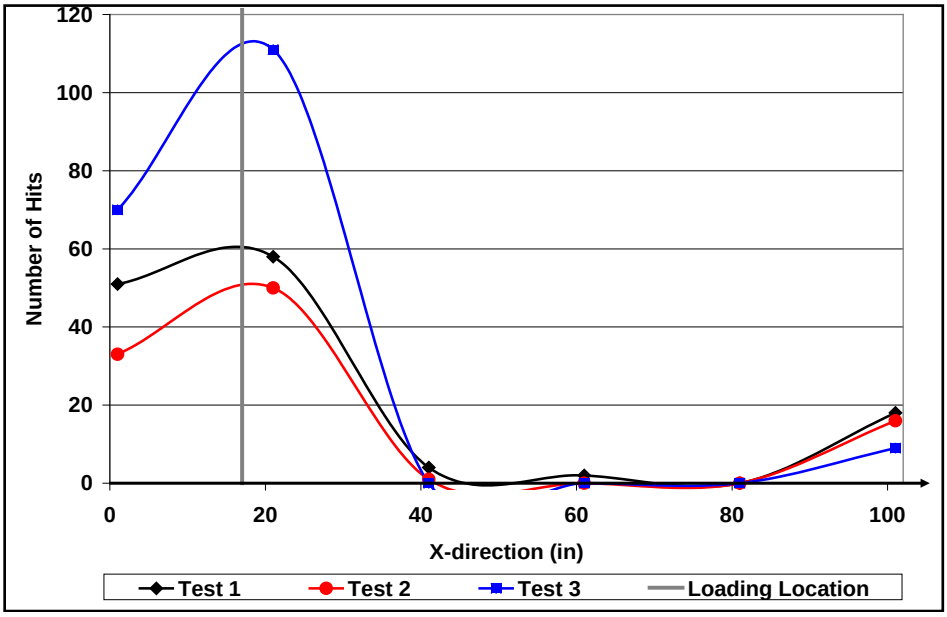

Figure 3.22: Number of Hits, Sensor Array 1; Three Tests Under 25 kips

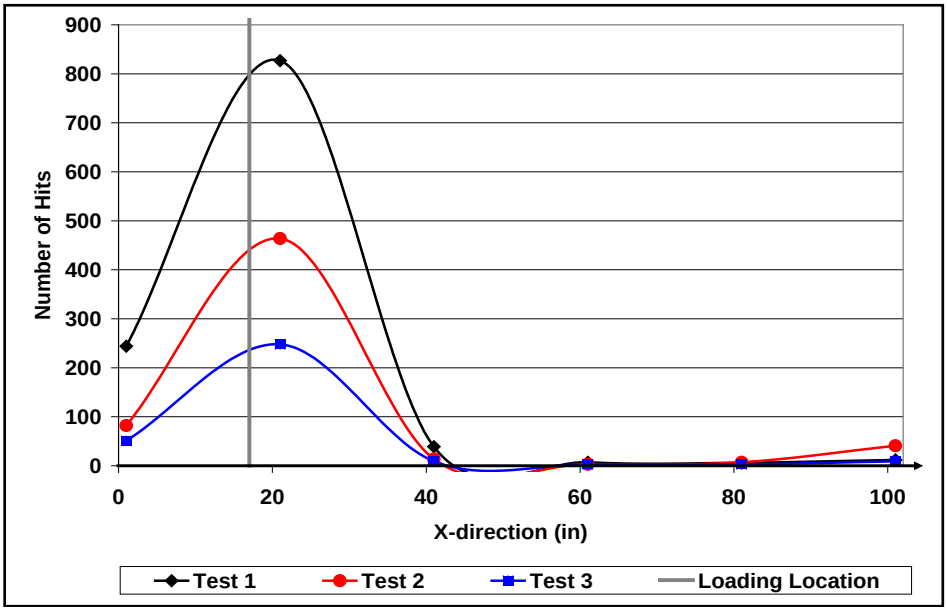

Figure 3.23: Number of Hits, Sensor Array 1; Three Tests, Over 25 kips

Repeatability of the findings is explored in the following sets of figures. In Figure 3.24 we can see that during the three test sessions, the values were similar and show the same general trend to demonstrate that the source location is generally near sensor S5. However, another pattern can be detected as well: the decrease of overall values. While each test has values that are similar, they decrease after the first analysis when near the source. As can be seen from the figure, at a distance from the source the values decrease until reaching the sensor on the opposite edge of the panel and do not follow any type of pattern, in that the highest values come from the third test and the smallest from the second, with the first test being somewhere in the middle.

Sensors closer to the source have somewhat of a pattern in magnitude. As the tests are performed, the values decrease, meaning that after the first test it would take more force to obtain values similar to the previous test, as shown in Figures 3.22 and 3.23. The occurrence most likely has to do with the panel cracking in places during the earlier tests that now have a lower stress from the same bending load being applied.

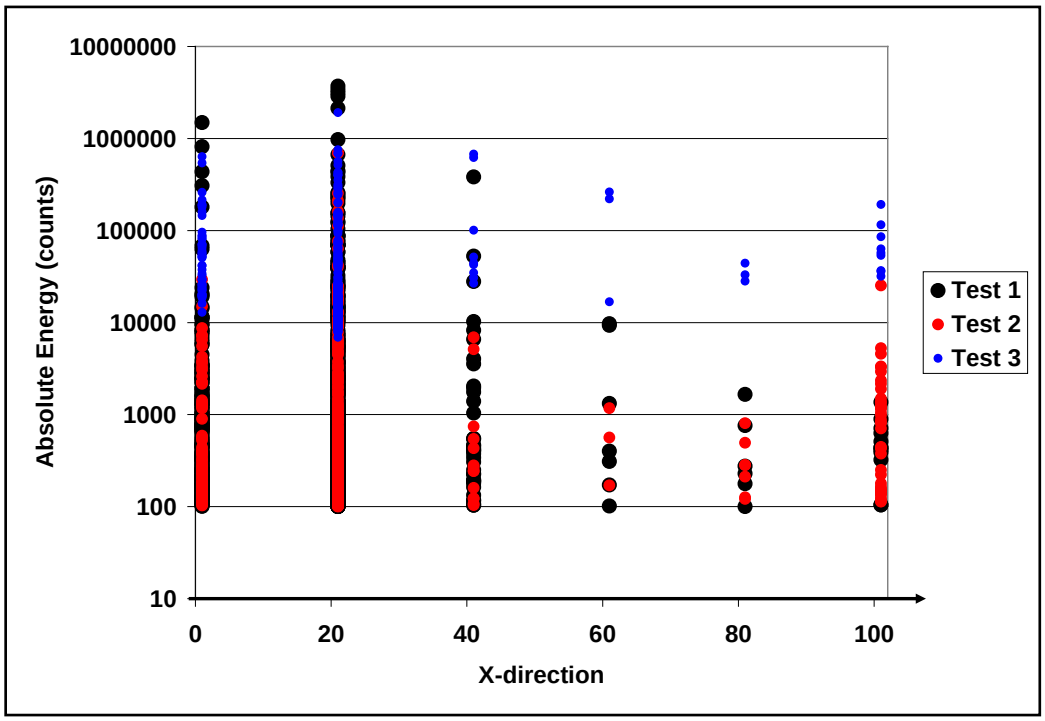

Figure 3.24: Absolute Energy Values Sensor Array 1; Three Tests

The last part of this section will demonstrate the usefulness of having the two arrays present during the testing. If we were to look at the first array without any knowledge of where the source was located, at this point it appears to be most likely between Beams 1 and 2, and closer to sensor S5 than to S2. And thus far this would appear be correct. But how would the source location be determined in terms of which side of the array the source is on?

In order to solve this question, the second array can be employed quite easily and effectively. When the second array is plotted with the first, as in Figure 3.25, a pattern emerges that shows that at distances farther from the source location, there appears to be a steady increase similar to both arrays, shown with the green line. The data from the sensors near the presumed source are more defined, and show that Array 1 has higher values than Array 2; therefore, the source would either be between the arrays, yet closer to Array 1, or on the side that is closer to the joint edge. While not a full network, the simple use of two arrays has narrowed down the location of the source to a fraction of the overall panel.

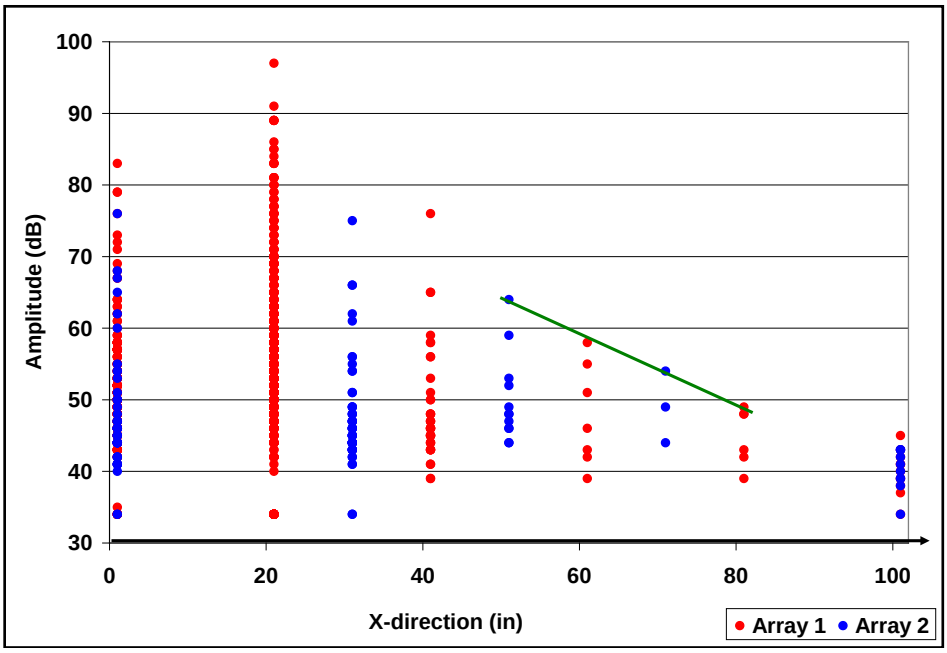

Figure 3.25: Amplitude Values Sensor Array 1 and 2

A further analysis of this technique shows that the number of hits recorded by each array is significantly different with Array 1 having a larger amount overall.

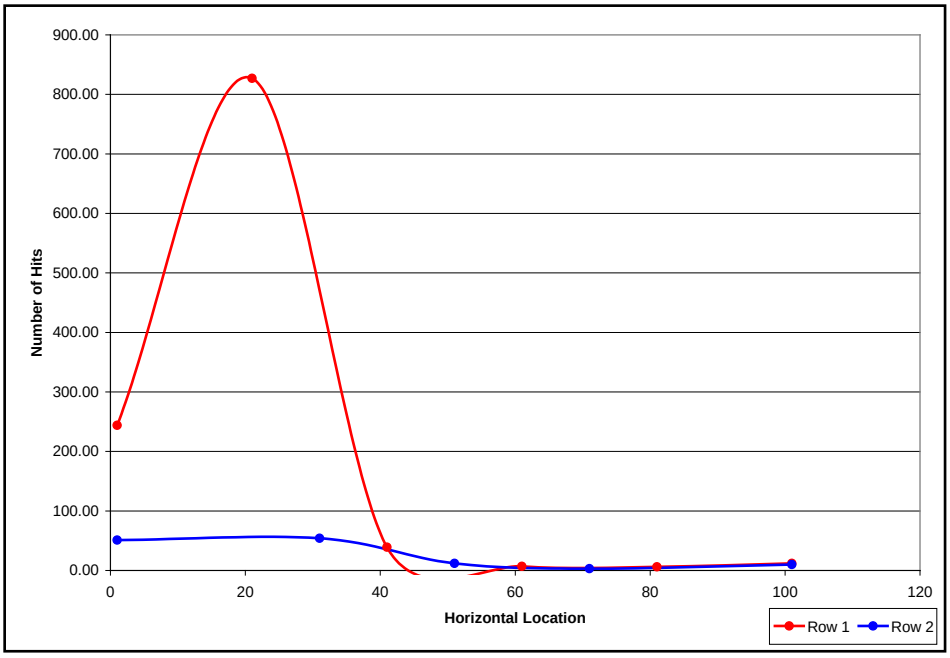

Figure 3.26: Number of Hits Across Sensor Array 1 and 2

Another phenomenon that can be seen from several of the previous figures is that the number of hits seems to decrease dramatically at around the 30-inch location, which happens to be near where a support beam is located. This decrease seems to be mostly from the lower energy and strength events, resulting in "small powered" fractures possibly going unnoticed across the beam. This means a set of arrays would need to be located between each beam if small energy events needed to be recorded.

3.4 Acoustic Degradation Analysis

By using the same data as in the last analysis, a pattern emerges in the values for energy and strength when plotted with relation to the distance of the sensor from the load. A decrease in the general properties is noticeable as the sensors are placed away from the source of the acoustic signal. This follows the same basic principle that was discussed by use of the arrays, but in this case the average values for all the data at a point are used, rather than just the high load time-

spans. This might show that if the average values for a network of graphs were plotted, the resulting chart might give the researcher a hint as to where further analysis should be conducted to determine if there is cause for concern.

The property that shows the greatest difference between distance points is that of the absolute energy as plotted in Figure 3.27. In this figure, we can see the decrease in magnitude as the distances increase. In this case the best plot was found to be that of a "Power Trend-line," which is not all that surprising as a great deal of acoustic properties have an inverted second-order relationship with regards to distance from the source. It appears in the case of AE in an FRP panel the relationship is no different, as that general trend exists here as well.

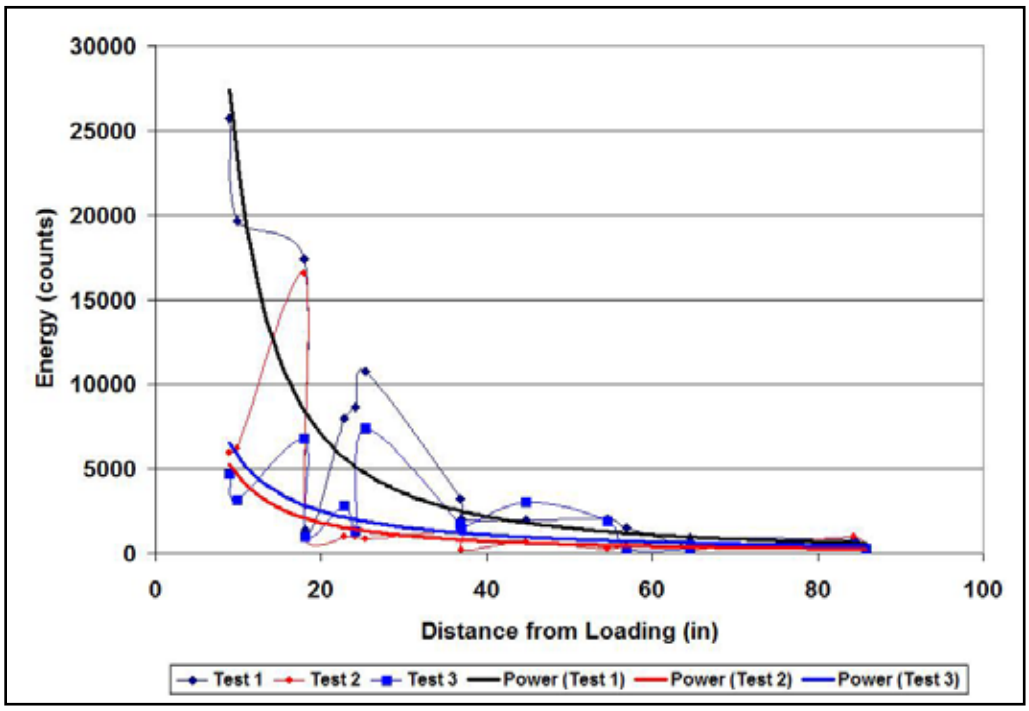

Figure 3.27: Average Absolute Energy Plotted at Various Sensor Distances

The next property examined is that of the amplitude data. From Figure 3.28 we can see that a similar trend is experienced as that in the energy plot in Figure 3.27.

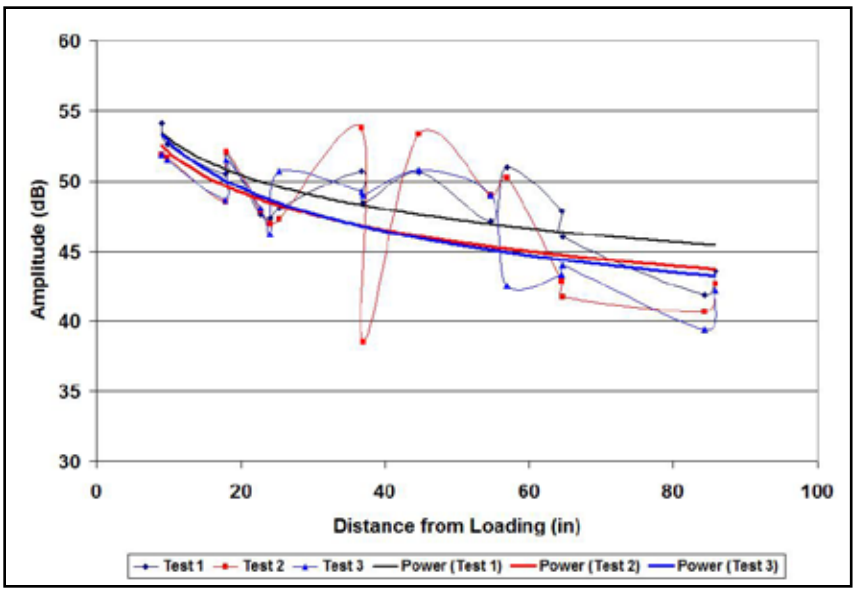

Figure 3.28: Amplitude Plotted at Various Sensor Distances

In all of the property graphs, the three tests plotted seem to show normalization to a linear relationship or nearly zero in regards to the distance after approximately 30 inches has been reached. This data strongly substantiates the determination earlier that sensors outside 2.5 feet were found to be much lower in both magnitude and amount of data recorded.

Given the information collected, a distance of approximately 1 to 2 feet should be observed when mounting the sensors on the actual bridge panels. This range would allow strong values to be recorded for the various signal properties when within the loading region, examination of the graphs, and the desire to have as large as possible an area covered by the sensor net. In the preceding graphs, the properties show a pattern of following the trend-lines up to 2 feet from the source and becoming erratic soon after this range has been surpassed. The interior limit was chosen due to large values being detected near the source, and the general idea that the sensors being too close together would be redundant and unnecessary.

The last analysis for sensor placement involved the use of the sensors on the top and bottom of the panels, as well as possible benefits of using one over the other. For this testing, the layout was changed once again to reflect the need to compare data taken on the panels' top to that taken on the bottom. This testing set has the force application applied directly to Panel-B,

while Panel-A records data from the transfer of the acoustic signal across the joint. The sensor layout designed and used for this analysis is shown in Figure 3.29.

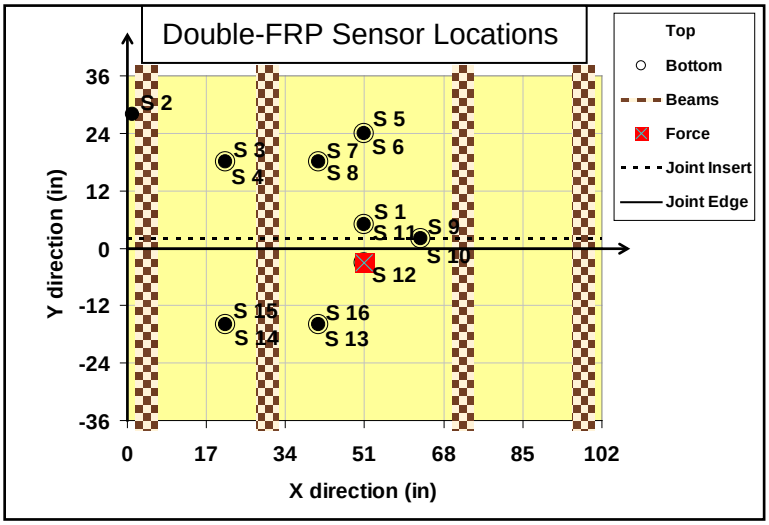

Figure 3.29: Degrading Signal Sensor Arrangement

Upon graphing the data, all of the sensors on top and within 2 feet of the force application location, situated over sensor S12, show a strong resemblance to their corresponding sensors located on the underside of the structure. The exception is sensor pair S13-S16, where sensor S13 detached partially from the panel before the silicone could set and record a proper response. Of the sensors outside the 2-foot radius, the S5-S6 pair did record data very similar to the S7-S8 sensor pair, located approximately 4 inches closer to the load, but all other sensor pairs recorded little data.

The closest sensor pair is S1-S11, which when plotted shows similar concentrations of data point peaks (Figure 3.30). The sensor located on the bottom of the panel, S11, has an increased number of data points and is most likely related to the interaction between the panel and support beams or the joint between panels. In this case, the latter would be more likely.

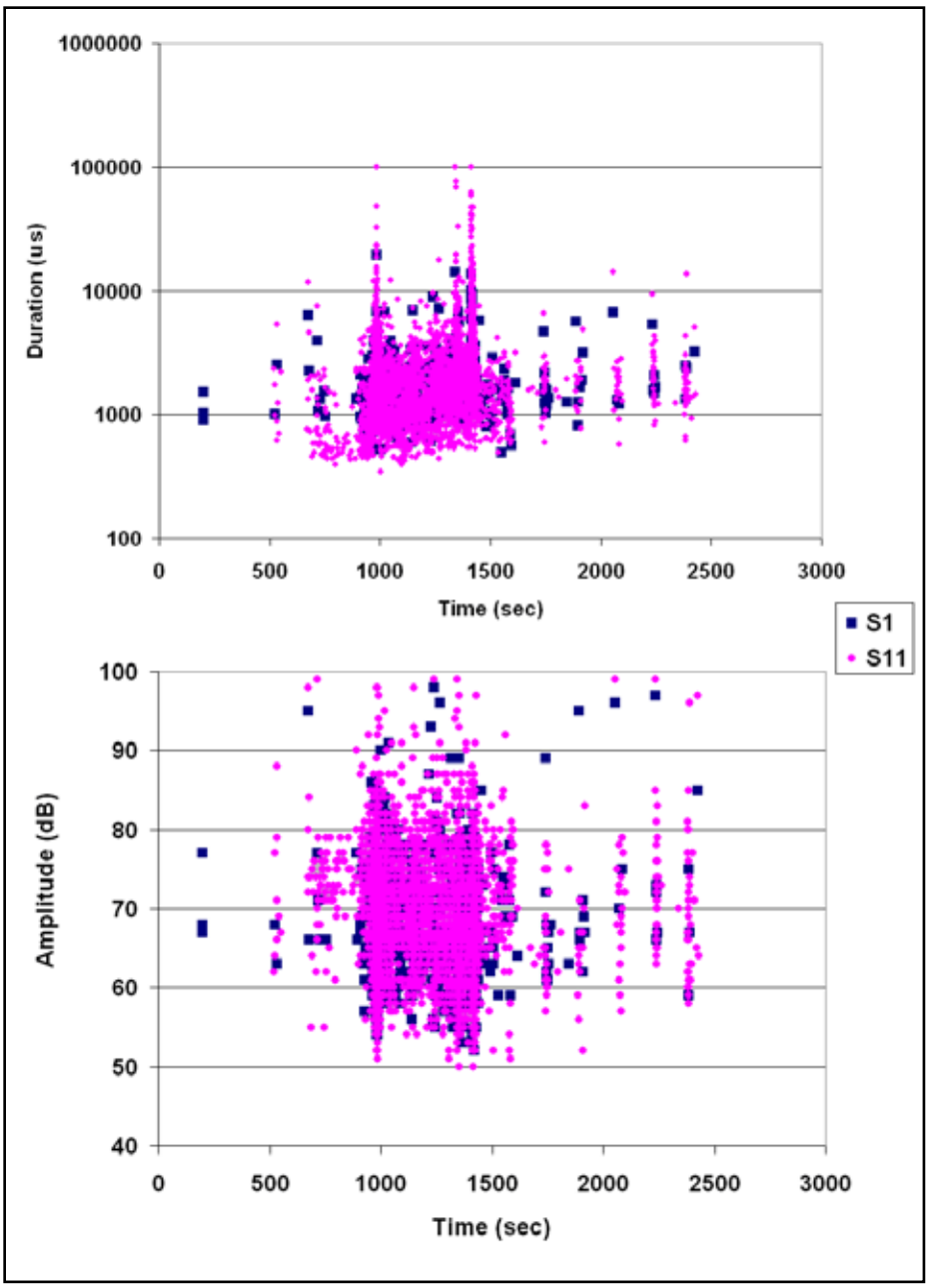

Figure 3.30: Duration and Amplitude Comparison of Sensors; S1 and S11

If the sensor pair S9-S10 is examined, a strong comparison can be made between the sets of data points. The individual sensor pairs can be seen Figures 3.31, 3.32, and 3.33. From the findings in this section, it seems that as long as the sensors are placed closer than 2 feet from each other and secured properly, it does not matter if the sensors are placed on the top or bottom of the structure overall.

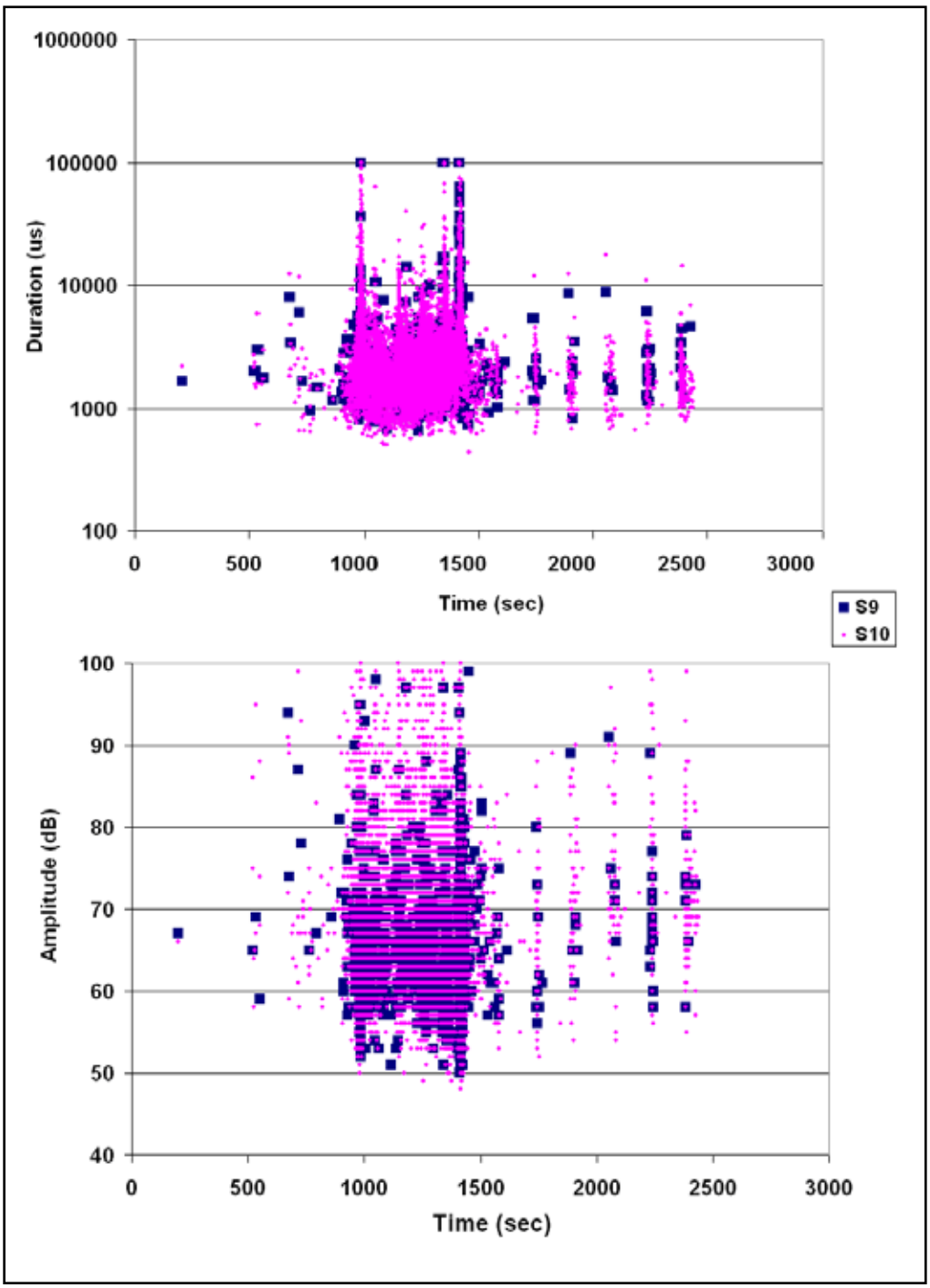

Figure 3.31: Duration and Amplitude Comparison of Sensors; S9 and S10

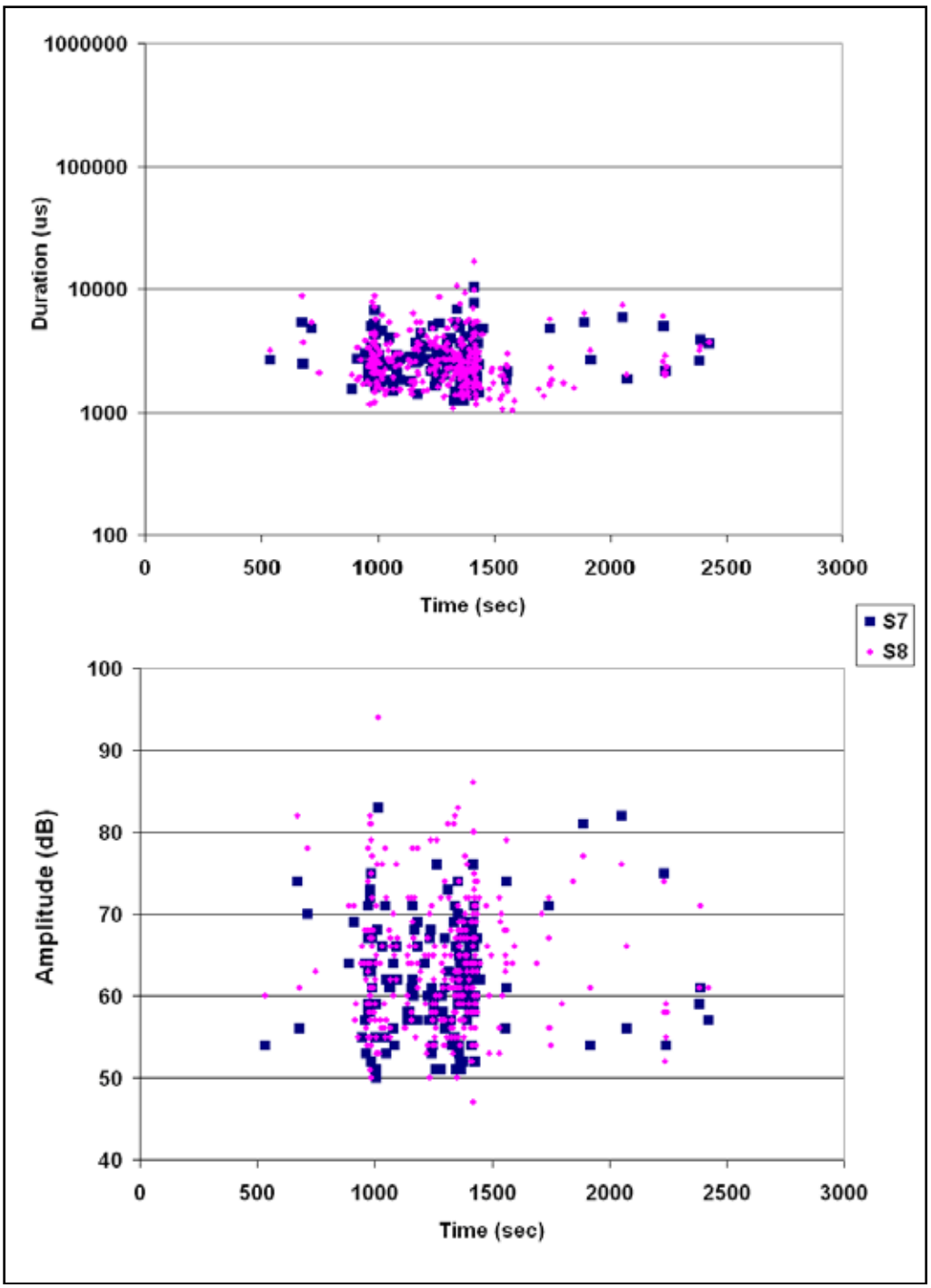

Figure 3.32: Duration and Amplitude Comparison of Sensors; S7 and S8

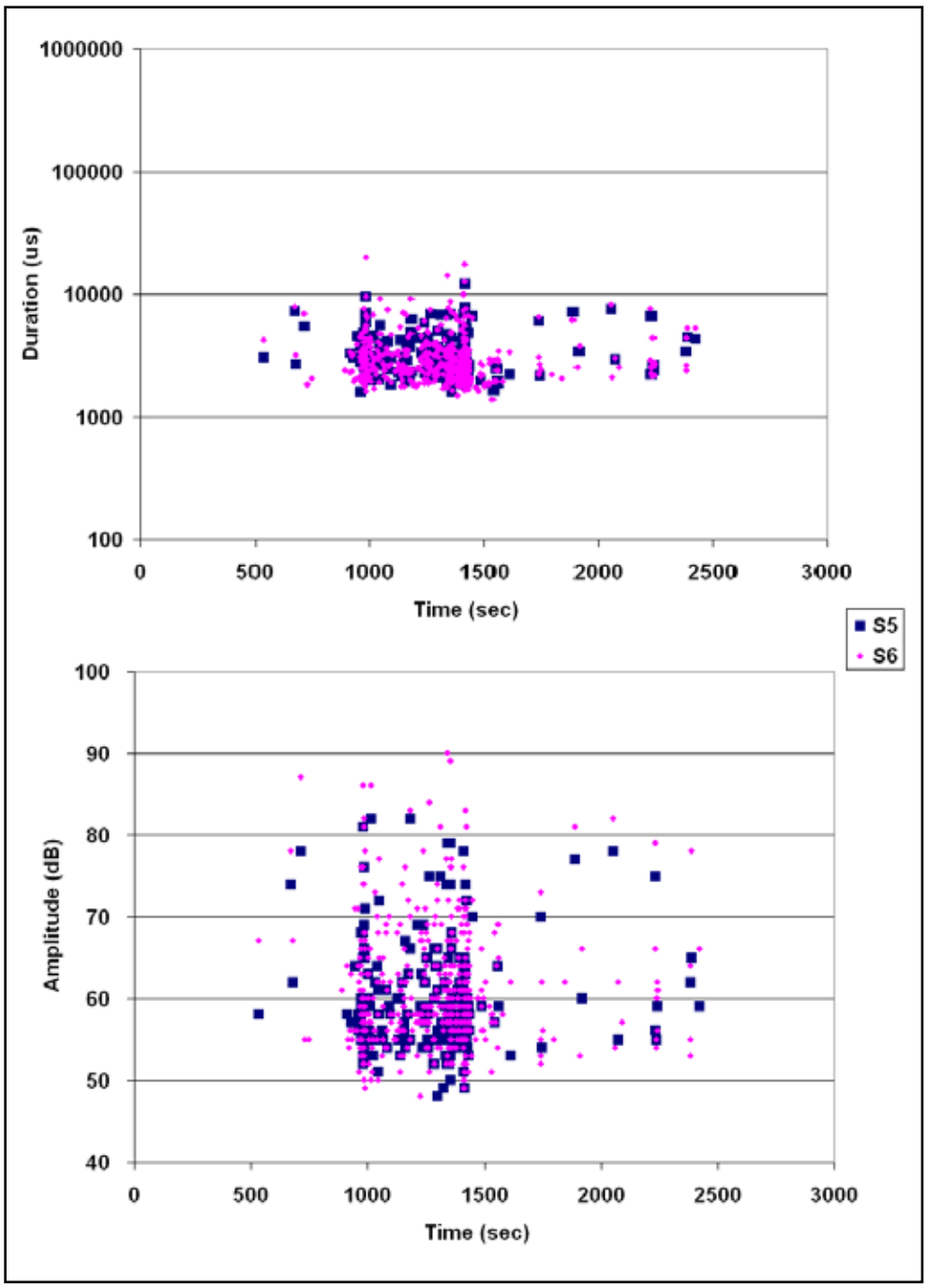

Figure 3.33: Duration and Amplitude Comparison of Sensors; S5 and S6

3.5 Signal Transfer in FRP Panels

One set of tests focused on analyzing performance along the joint with the force application location, specifically at the middle of the first beam on Panel-A. The sensors were positioned in locations that would result in similar distances from the force being applied, but

located on separate panels, as shown in Figure 3.34. By this method, a general profile should become apparent as to how well the acoustic data transfers from one panel to the other.

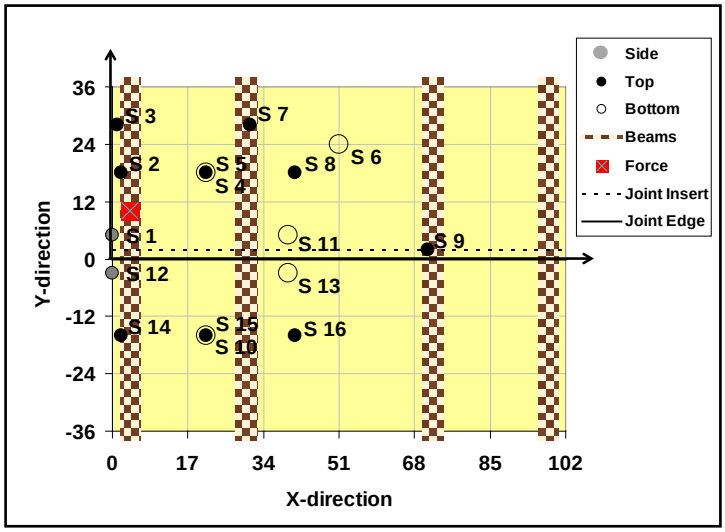

Figure 3.34: Signal Transfer Sensor Arrangement

During the setup process the sensor placement was originally intended to record data for a force located on the crack itself. However, upon further planning it was determined this would not work appropriately. The force would cause acoustic data to occur in Panel-B not just due to transfer from Panel-A, but due to a force transfer through the material touching the lip to come under stress and possibly experience some inadvertent bending forces. This would result in a large amount of sensor readings coming from the lip of Panel-B due to the nature of the lip-and-groove connection. Due to multiple likely acoustic source locations, the overall effectiveness of the study would be diminished and possibly useless.

Another concern is damaging the panels. While one of the panels is eventually damaged at the end of this project stage, it is not the goal of this investigation to damage any of the panels unnecessarily. The lip could likely experience bending that would result in damaging the structure so that the joint would have to be repaired before further analyses could be attempted. Additionally, the load could simply break the lip off of Panel-B without an adequate substitution ready for testing within a satisfactory time frame.

Instead, the load was kept in a location approximately 10 inches from the joint edge, and placed over the first beam. The sensors were then compared to one another based off their general location on the structure over a series of three tests occurring in the same arrangement. For example, sensors S7 and S15 are located approximately 32.5 and 31.5 inches from the source and are on separate panels. The resulting graphs would therefore be expected to be similar if the joint does not create a problem for acoustic transfer between the panels. Three other pairs of sensors are located at points that are acceptably the same in distance from the source, having less than 2 inches of difference. They are S6-S16, S7-S10, and S11-S13.

The comparison between S6 and S16 is basically non-existent. After the data has been filtered and plotted, there is almost nothing to compare between the sensors. While there is some information that is similar to each other in the S7-S15 comparison, the vast majority of data points graphed do not lead to a good comparison between the sensors. These results are most likely due to the distance between the loading source and the sensor locations, over 2.5 feet away in all cases.

The S7-S10 comparisons have an interesting problem of their own, where the S10 sensor records large amounts of data while the other does not. The sensor designated S15 does not receive as much data as the similarly distanced S10 either. The most likely cause for this is that the sensors located on the bottom of the panels at a moderate distance from the loading source may be detecting noise created from the panels interacting with the beams they are supported with. This is most likely due to localized matrix cracking and possibly rubbing or movement between the panels and beams. Representative graphs for the S7-S10 comparison in terms of absolute energy and signal strength can be found in Figure 3.35 and Figure 3.36.

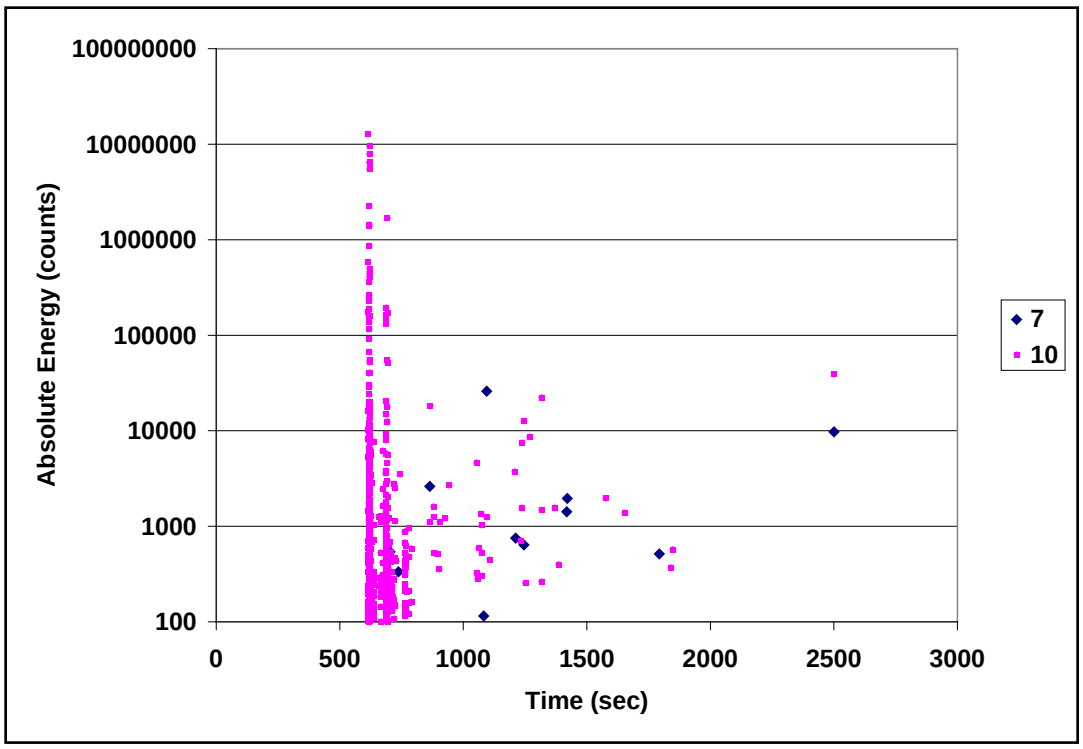

Figure 3.35: Absolute Energy Comparison of Sensors Located Equidistant from the Source; S7 On Top of Panel-A and S10 On Bottom of Panel-B

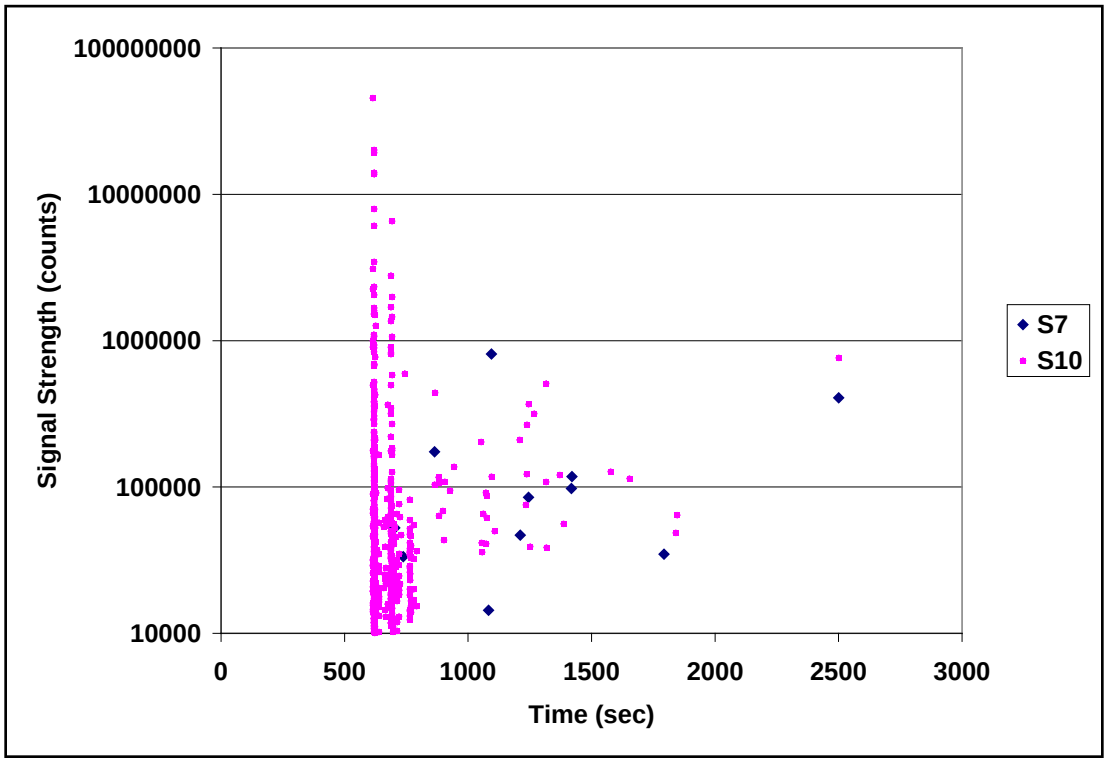

Figure 3.36: Signal Strength Comparison of Sensors Located Equidistant from the Source; S7 On Top of Panel-A and S10 On Bottom of Panel-B

The last set of sensors provides more useful data in which a clearer pattern can be seen in Figure 3.37. However, the extreme closeness of the two sensors to one another and proximity to the joint in general may be the overwhelming cause of these results. Any movement experienced between the panels could create an acoustic event, and therefore both panels would transmit the signal through themselves and to the sensors, but not be a transfer from one panel to the next.

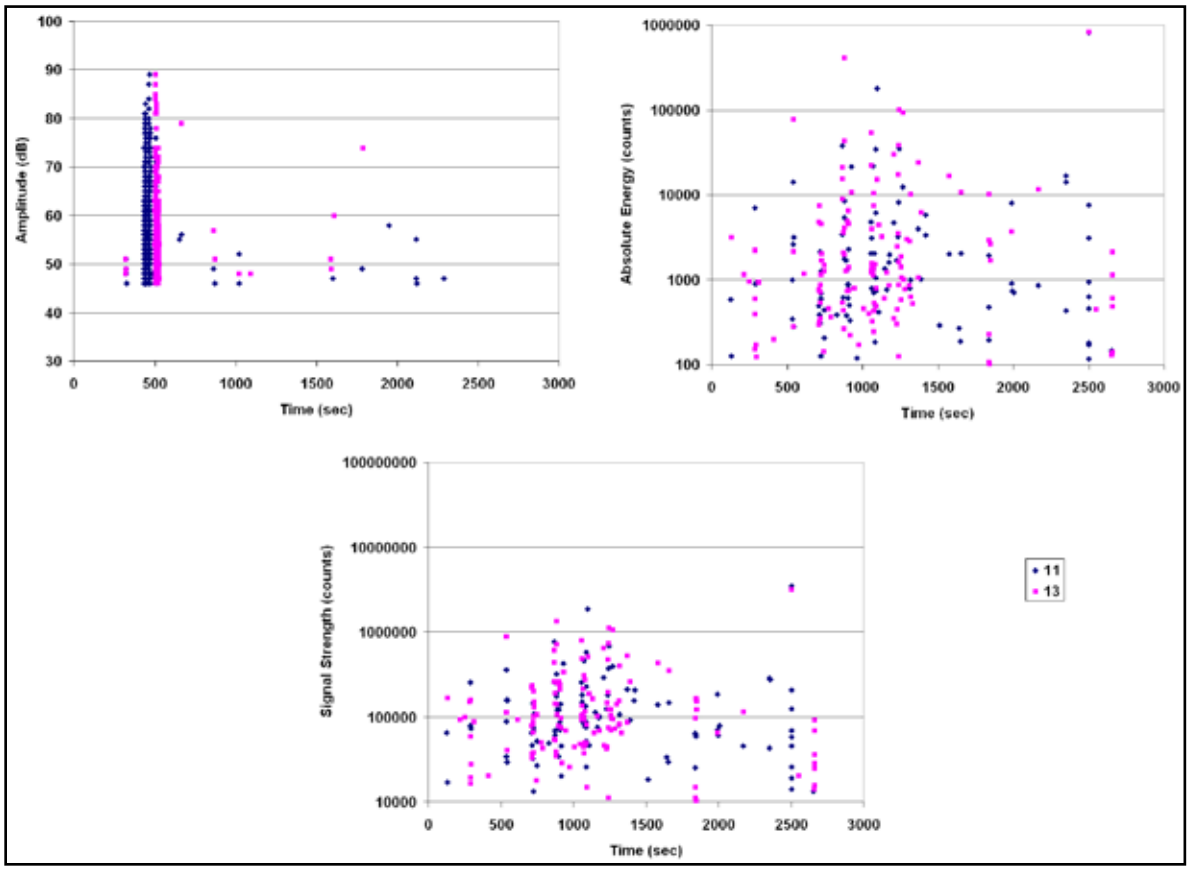

Figure 3.37: Amplitude, Absolute Energy, and Signal Strength Comparison of Sensors Located Equidistant From the Source; S11 On Panel-A and S13 On Panel-B

Due to the uncertainty of these results, the force location was moved between the first and second beam. This change in location, though short, creates a greater bending force in the panel, and therefore should create more acoustic emissions from material failure. The change in location also makes it so three sensors are spaced approximately the same distance at just over 2 feet away. Sensor locations S3 and S8 were located on Panel-A and S15 on Panel-B could be used as the comparison sensor for signal transfer. The resulting graphs show some correlation,

indicating that the decrease in distance between the sensors and the loading application location does create readings that are both clearer and more comparable to one another. Figure 3.38 shows that while sensor S15 still recorded more data than the other two, all three had data points that increased and decreased together, especially for higher valued points. If examined closely for each higher value from sensors S3 and S8, there is a value relatively close from sensor S15 as well.

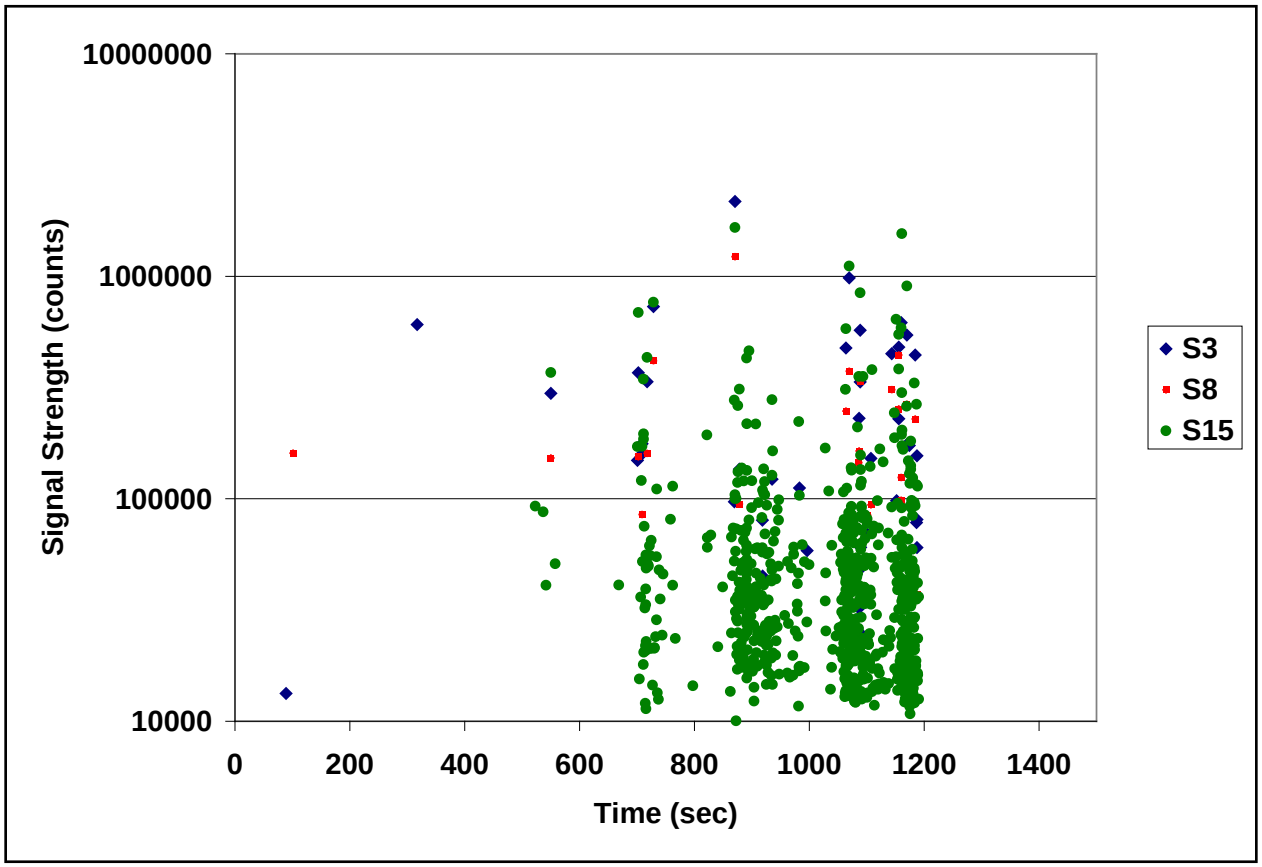

Figure 3.38: Signal Strength Comparison of Sensors Located Equidistant From the Source; S3 and S8 On Panel-A and S15 On Panel-B

From the testing results, it seems that while "low powered" acoustic events can create hit points within their own panel, ones with greater energy and overall strength can be recorded by monitoring devices in adjacent panels. At least this has been shown to occur in cases when the sensors are within a close range to the source in other panels.

3.6 Single Panel Failure Event Analysis

Near the end of the testing a few follow-up tests were being conducted on the single panel, which inadvertently became an opportunity to analyze some failure data for the internal structure of Panel-A.

3.6.1 A Single Panel Analysis: Leading to Failure

A force was being applied to the center of the panel at locations on and between beams located horizontally from the force application point designated in Figure 3.39, which is placed at the location where the failure occurred. The two preceding tests occurred centered over Beams 2 and 3, respectively, but no information was recorded that hinted at the upcoming failure. In fact, there is very little acoustic data at all from the test over Beam 2, even without using the signal strength and energy filters. The test from Beam 3 contained more data but not as much as in earlier tests, indicating that even in this analysis very little occurred in regards to acoustically significant events. After the failure occurred, an earlier test was reexamined to determine if any earlier signals were present to signal the oncoming event.

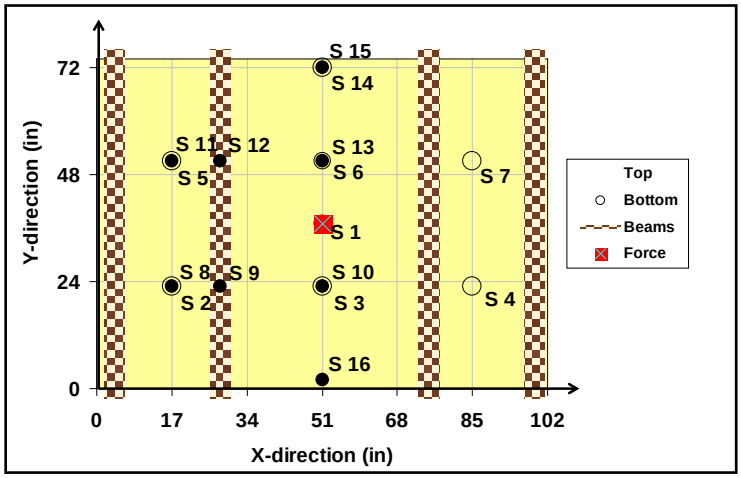

Figure 3.39: Final Sensor Location Layout

When the hits are plotted on a Duration-Amplitude graph for the data from the test over Beam 3 (Figure 3.40), the hits barely get into the upper third of the graph, and are predominantly centered in the section designated for low-amplitude matrix failure. There seems to be no

indication of fiber failure or any major structural problems by use of this method; however, with the beams located under the force application locations, the structure is subjected to more of a compressive loading rather than a bending loading as when the force is between the beams.

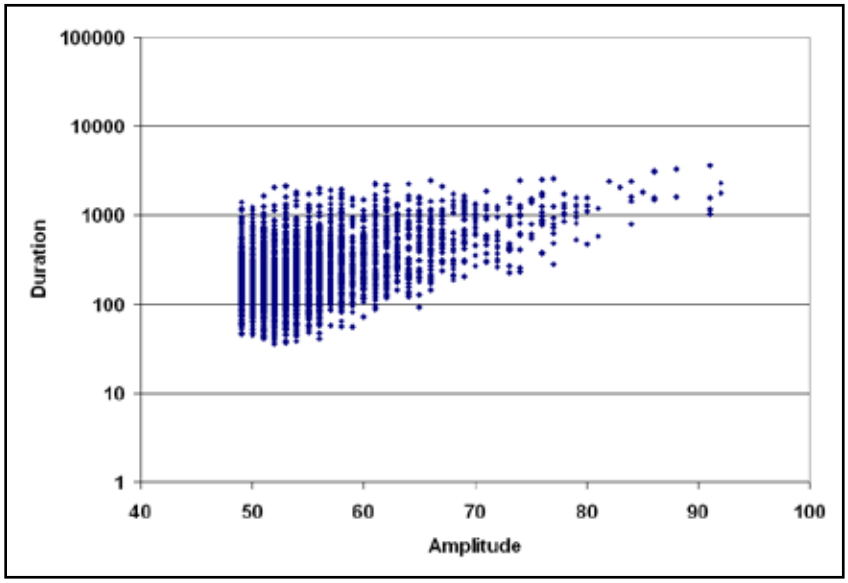

Figure 3.40: Test Over Beam 3, Duration-Amplitude Graph

At this point, a closer pre-failure analysis was done on the last test to be conducted between the second and third beams; however, this took place only 10 inches from the joint edge, not actually at the failure location. Also, the sensors were set up in the configuration presented in Figure 3.18. While there was no analysis performed with sensors located at the failure area, and no other test involved the force being applied at the center of either panel used, this data could still give insight as to whether there is any increased risk to having the force applied between the center beams. In Figure 3.41, the Duration-Amplitude graph shows that a large amount of the data points are once again mostly located in the "Matrix Failure" area of the graph, but also has a healthy amount of hit points in the region previously designated for "Crack Growth" (Figure 3.2), and seems to come from a sensor located closer to the center of the panel in the X-direction.

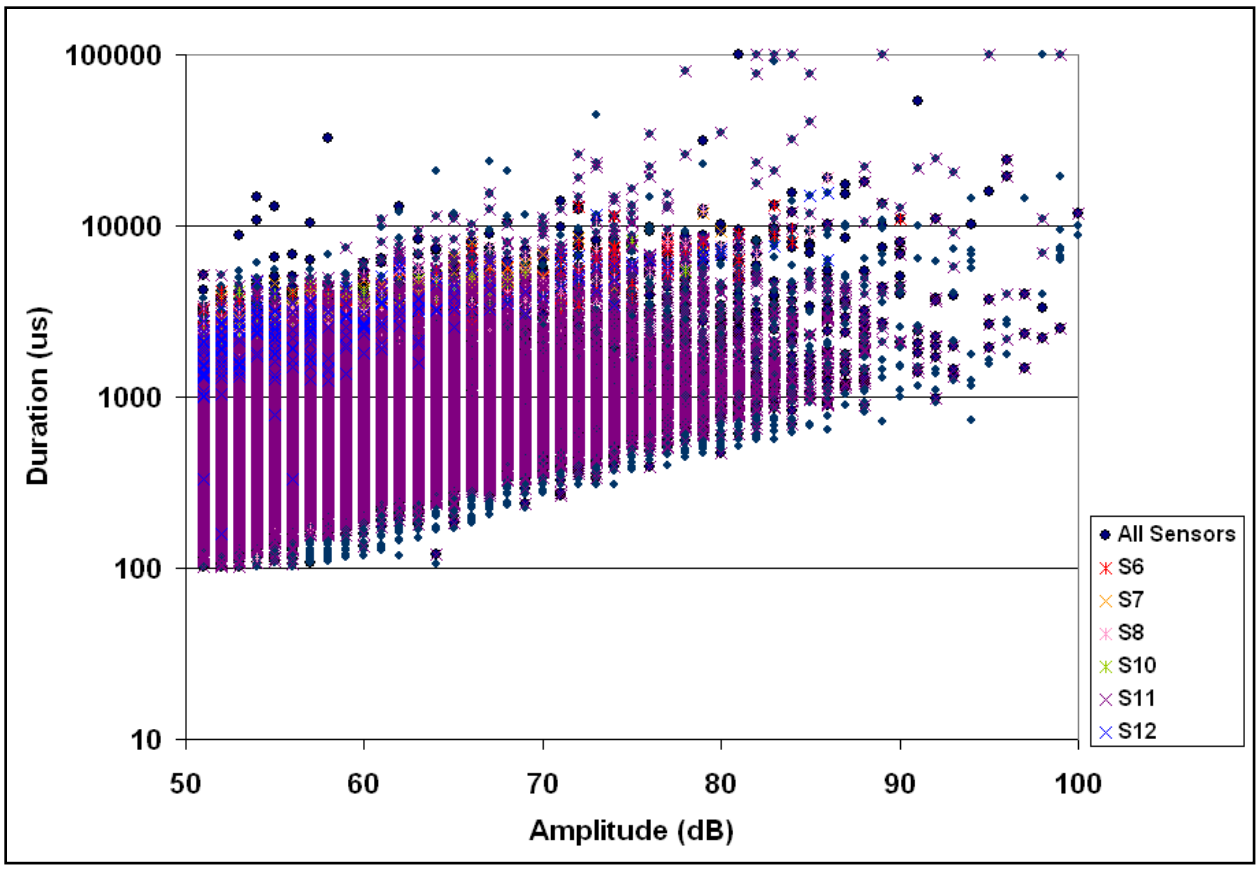

Figure 3.41: Duration-Amplitude Graph of Test on the Joint Edge Between Beams 2 and 3

From this and earlier charts, there is some indication that there was little fiber breakage within the structure during the tests regardless of force location. The overwhelming majority of the events seem to indicate that there was some early matrix cracking and growth that only increased when the tests got closer to the center of the panel.

3.6.2 Panel Failure

The initial procedure for the test was conducted similarly to those performed earlier, with a gradually increasing step method. The loading was being applied in steady increments and the peripheral devices were functioning normally. After holding at around 20 kips for approximately 2 minutes, the load was manually increased until 27 kips was obtained. The load was held steadily for approximately 1 minute, at which point audible sounds began emanating from the structure and a sudden decrease of load was recorded. The load then quickly spiked as the cylinder was being controlled by the user, but was then removed from the structure. The selected

loading cycles and amplitude data are presented in Figure 3.42, while energy and duration can be found in Figures 3.43 and 3.44.

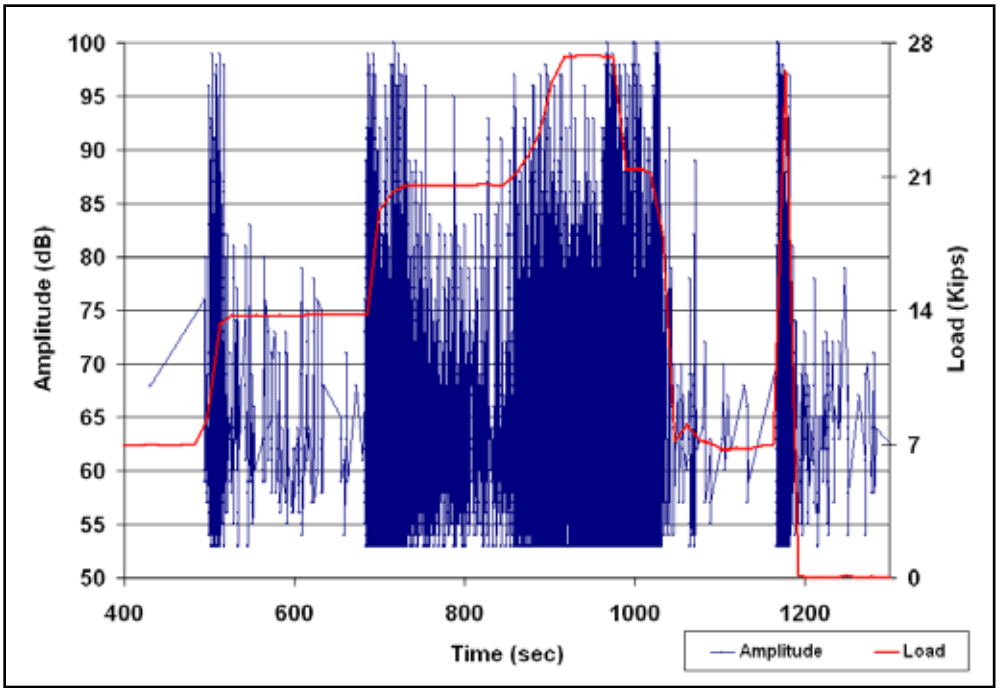

Figure 3.42: Failure During Test, Amplitude with Load Overlay

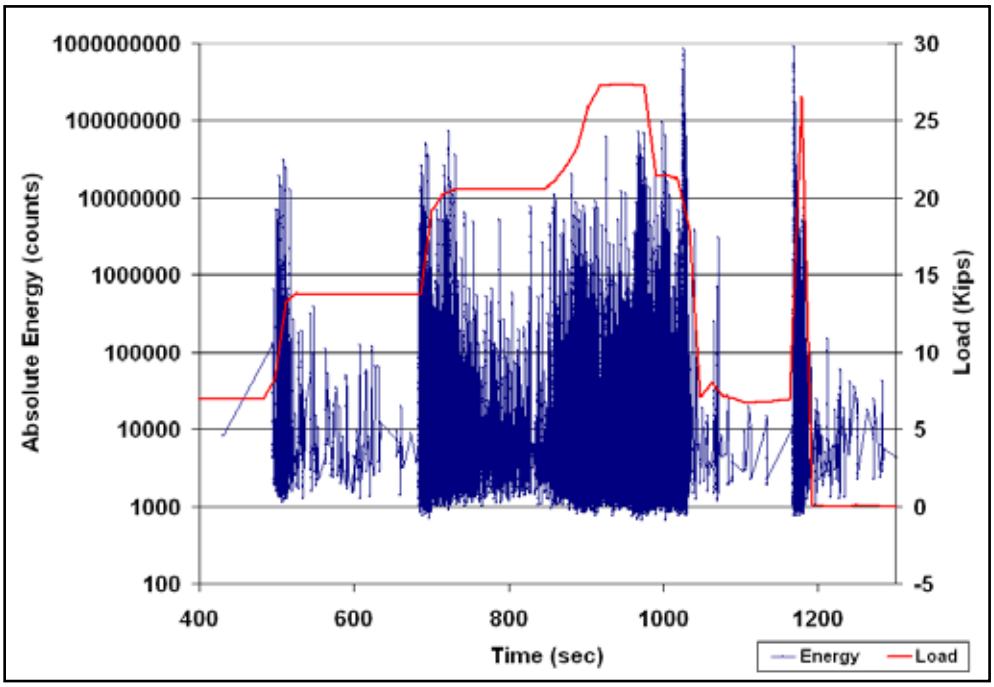

Figure 3.43: Failure During Test, Absolute Energy with Load Overlay

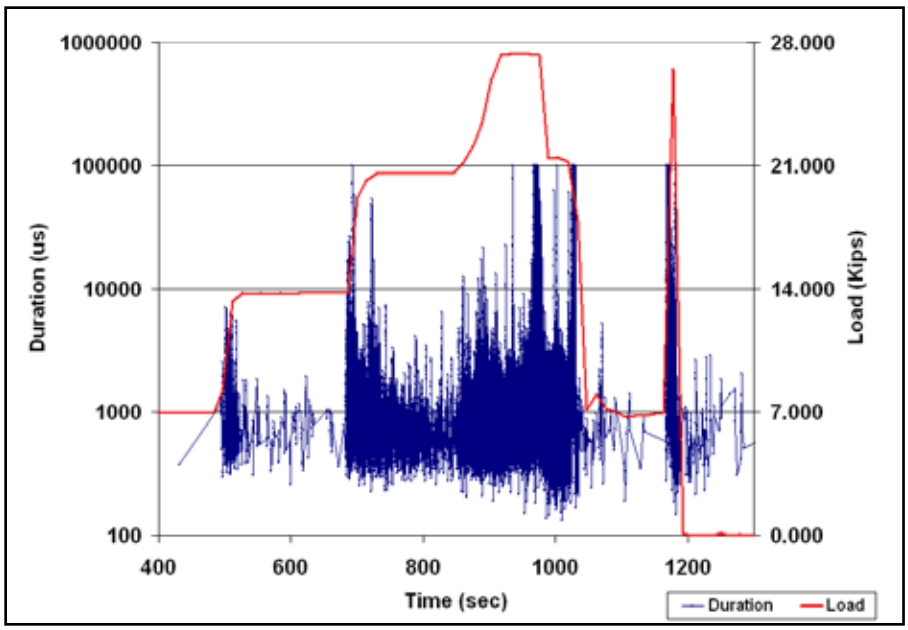

Figure 3.44: Failure During Test, Duration with Load Overlay

The cause of the failure was initially unknown and no signs of failure were exhibited on the structure exterior. Subsequent examinations showed that the load likely caused damage to the interior structure, crushing of the core, which was further shown to be the most likely occurrence when the normal load was reapplied and the pad actually "sunk" into the surface of the panel by about an inch.

Before the failure occurred, there was a significant difference noted in terms of the AE property responses during the increase in load performed before the failure and all earlier increases in load. As can be seen in the previous figures related to this test, when the load increased there is no sudden spike of activity as had occurred in nearly every examination up to this point. Instead, the values slowly increased in response to this new load and do not show nearly as much change in magnitude as in earlier tests. Upon reaching the new load, the property magnitude does not seem to decrease, but remains at about the same level up until the failure. Another occurrence is that upon reaching the maximum load, the magnitudes receded briefly and proceeded to increase again right before the failure occurred.

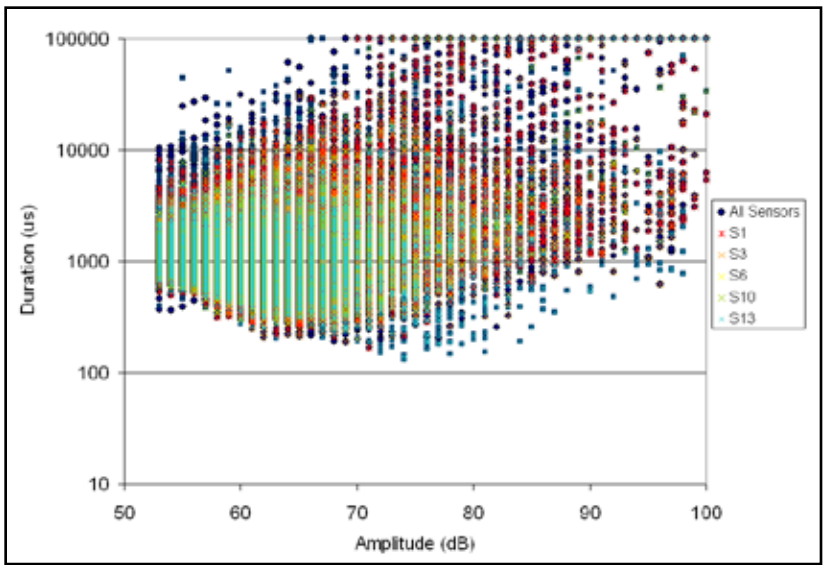

Figure 3.45: Duration-Amplitude Plot of the Failure Test

From the Duration-Amplitude graph displayed in Figure 3.45, we can see that there was a large amount of mid-amplitude, high duration hits recorded during the test. As with the analysis of the earlier test conducted between the two interior beams, this has been found to correlate to matrix cracking and delamination between the fiber layers. Also noticeable is a lack of high-amplitude, high duration hits, meaning that the most likely cause of the failure is due to the matrix failing.

The individual sensor data on the plot of Figure 3.45 to some extent show that the closer to the event site the sensor was, the more it recorded “Fiber Breakage” region failure on the graph. This indicates that while matrix failure occurred in the area around the center of the panel, the majority of the fiber failure was constrained to the epicenter of the event.

If the charted hits are separated differently, it becomes apparent that a large amount of the data collected occurred when the applied load reached its maximum value, creating a resulting stress that caused the matrix to crack and the overall structure to fail. Figure 3.46 implies that during the maximum load, a concentration of acoustic data is once again formed in the center of the graph designated as “matrix cracking” and “crack growth.” These displays imply that the majority of the acoustic data occurred during the maximum loading cycle prior to the failure, most likely due to failure of the bond between the core and the structural surface leading to an

overall matrix failure in the core material near the load source. Many of the hits in the fiber break region apparently occurred during or after the main failure, most likely due to structural collapse of the core material discussed previously, providing interior structural support.

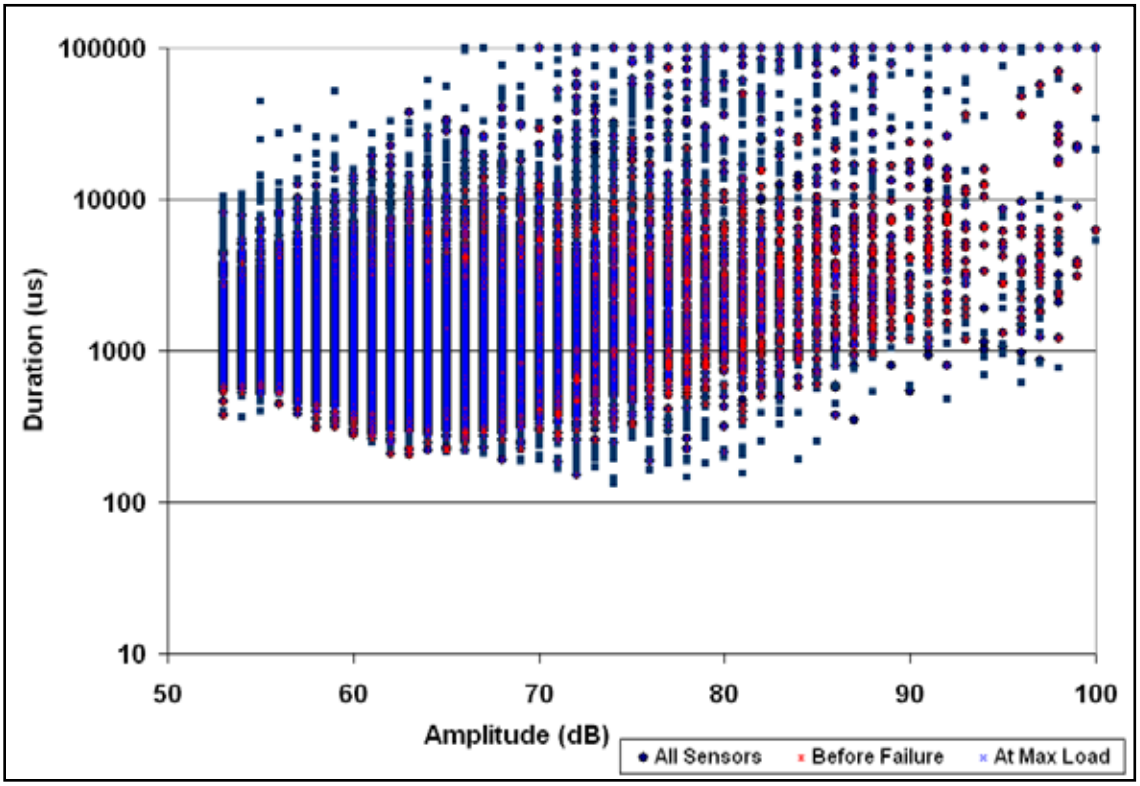

Figure 3.46: Pre- and Post-Failure Duration-Amplitude Plot of the Failure Test

3.7 Long-Term Monitoring

In preparation for the next stage, the groundwork was started in making this system completely wireless so that long-term monitoring can be conducted without the need to go to the monitoring site to gather the data. In order to make the system more flexible in its application and use, the monitoring device will not use a land-line phone or power lines. The lack of wiring should allow the system to be placed in nearly any location on a bridge structure. The power requirements for the system and the modem are planned to be generated by the use of solar energy and a regular car battery storage cell as shown in Figure 3.47.

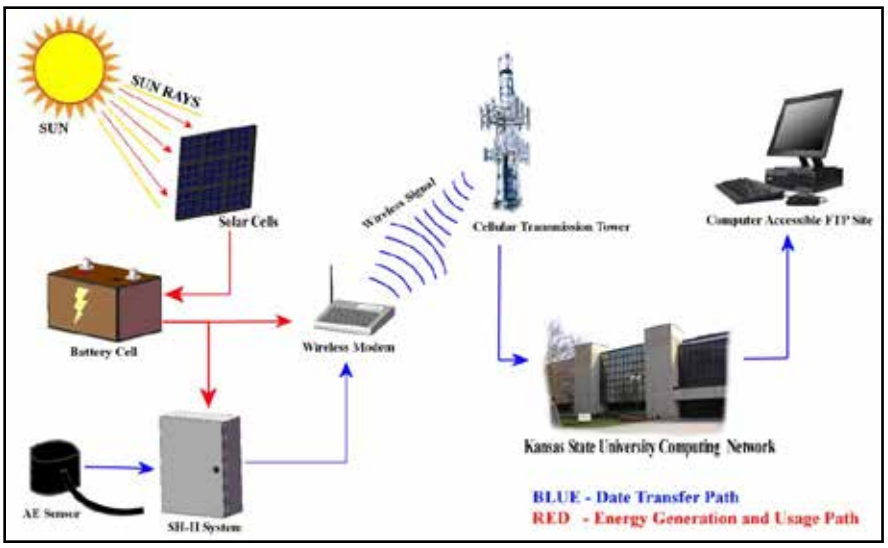

Figure 3.47: Monitoring System's Power and Data Flow Chart

The data transfer will be conducted through the use of a modem that has been integrated into the SH-II system itself. Upon data collection and applying the filtering process, the data will be stored in the flash memory until a designated time each day when the contents will be sent to Kansas State University for processing. At a designated time, most likely to be late-night, the system will "dial up" access to the internet and access a secure FTP site on Kansas State's campus. Upon contacting the site, the contents will be uploaded from the system, subsequently purged from the flash card's memory, and disconnect from internet access. At this point the system has performed all necessary duties for data upload and continues to record data as normal until the next data uploading. The system can be set up so that if a connection cannot be made for whatever reason, the system will not delete the data, but retain it until the next uploading cycle is reached.

The data can be stored on an FTP site on the Kansas State Computing Network, and since this is a secure network, the files are at little risk of being accessed, deleted, or tampered with by other means from outside sources. This also means the only way to access the data is from on Kansas State University's Manhattan campus, and while this option still has limitations, it is much more practical than manually downloading the data from the system directly.

Chapter 4: Summary and Future of Research

4.1 Summary

From the summer of 2007 to the spring of 2008, tests and analyses were performed on FRP bridge decks at Kansas State University. The applied specimens consisted of two panels of equal size and structure with acoustic sensors and strain gauges attached in various locations to detect loading effects. A variety of properties and sensor presets were used to determine how the sensors should be used in future FRP panel analyses and similar applications. The gathered data consisted of a variety of results and provided significant insight into how the panels would function and possibly fail in actual use.

Based on the analyses conducted during this project, a variety of conclusions can be made from the results determined and included in this report. These include:

1. While not initially intended to be tested for, the majority of the results show that the panel is capable of resisting long-term damage if a load over 30 kips occurs for at least a short period of time. However, repeated occurrences could affect the interior structure and eventually lead to localized failures.
2. Thresholds are necessary to keep unwanted data from being recorded. This includes machinery and environmental background noise which seems to usually occur below 45 dB. The analyses showed that additional thresholds could be applied without sacrificing important data, including up to a 60-count energy threshold.
3. The Amplitude-Duration Graph does seem to work well in categorizing the data in terms of what caused the acoustic signal and indicated that there were definite regions where varying types of source failures show up on the plot.
4. When a load is first applied, it results in increased magnitudes of Amplitude, Energy, and Signal Strength. These values quickly decrease after the desired load has been achieved, but do not return to the earlier values. Instead they remain at an increased state until the load is decreased, at which point a smaller spike in magnitudes sometimes occurs, but it then drops as expected with the load.

5. Repeated loading cycles occurring in the same panel location indicate there is a decreased magnitude in reference to the values displayed during dynamic loading changes, while static loads appear to have similar values in each analysis.
6. Individual sensors have a range of up to 2 feet for gathering acceptable data. The decrease in property values appears to have an inverse correlation to distance as well as being a second order relationship. This is similar to the activity of past analyses and the overall accepted behavior of acoustic related properties, which equations are typically based on inverse second order equations.
7. While acoustic data does travel through the joint, it is unclear how much it affects the signal. The limit of a sensor to be within 2 feet of the source makes it difficult to examine this property more. This is due to the increase in acoustic signals recorded due to plate contact effects in the sensor. The sensors detect the response of the joint as well as signals created in both panels when the force applied is near the joint. These problems make it nearly impossible to accurately gauge the signal transfer from one panel to the next.
8. Sensors placed on the underside of the panels can accurately record the data produced in comparison to the sensors on top. There is typically a marginal increase in acoustic activity detected by the bottom sensors, most likely due to the support beams.
9. Panel failure type can be, at least in part, determined by use of the Duration-Amplitude graph, by looking at what region has more acoustic activity occurring at the time.
10. The most likely form of panel failure will come in the form of matrix failure from within the structure. When a force is applied to the outer layers, they tend to provide some resistance to the force, while the inner structure is incapable of providing the same. Due to this property, the inner layers tend to buckle and fail through means of matrix failure and compressive forces.

4.2 Future Work

The way in which a panel fails still needs to be examined more closely. In previous projects, the goal has been to design a panel that could handle bending loads and further the ability of a FRP panel to work under higher loadings. In this project, the failure properties of the previously designed structure were touched upon briefly and by accident. A detailed examination of what signals are produced prior to and during a failure should be conducted to help predict a failure before it happens.

While the classifications on the Duration-Amplitude graph developed in the earlier project stage seem to be generally accurate, a more detailed evaluation could also be performed. This would provide the monitoring personnel a better understanding of what is happening on, and more importantly, in the panel structures.

Additional studies should be conducted into the thresholds applied to the sensors. While some have been utilized in this project, there are most likely more exact values and properties that could be utilized to increase the efficiency and accuracy of the monitoring device.

While a signal location property of the software was utilized in this project, it was not utilized to a great extent or included in this report due to the production of obvious results. Due to the nature of the testing procedure used, the acoustic source location nearly always related back to the sensor nearest to the force application location. While this is good, and shows that it works properly, there are no alternate possible sources anywhere on the structure. If there was a possible way to load on multiple locations it might be interesting to research how the structure responds and how the location software performs in such a situation.

In relation to that, if these structures are to be widely used as a traffic bridge it might be a good idea to apply loads that reflect that environment more. For instance, developing a testing setup that would have a “driven load” wheel go across the surface to determine what effects a dynamic load might have. The location program could then be tested in an environment that has an increased number of properties, and determine where “problem areas” might be located in the panel structure as a vehicle travels over the panel.

An analysis as to how the beams interact with the panel structure could provide insight into how the distance between the support beams affect the acoustic data and the bridge

structural capabilities as a whole. This is only mentioned due to the lack of any failure characteristics being present between Beam 1 and Beam 2 in comparison to Beam 2 and Beam 3, Beams 2 and 3 having the longer span. However, this failure between Beam 2 and Beam 3 is more likely to have been due to poor construction, as in previous testing of longer spans no failure was noted at more than double the loading. These locations are also suggested to be where the sensors should be more closely monitoring the panels. The bending stresses created by a downward force, in addition to being the more weakly supported section of the panel overall, makes these locations a more likely target for the failures to occur.

Sets of arrays in two directions would also help in locating problem areas. While two arrays were able to locate a relative position in the X-direction, having arrays in the Y-direction would most likely yield similar results. These two sets of information together would be very useful in narrowing down the failure location to within a few feet on panels of the size used in this analysis stage.

Finally, when the analyses are being conducted on the bridge, the data should initially be compared on a daily basis to examine what changes occur while the bridge connections and bearings are settling into position. As shown earlier, a panel seems to change in regard to its acoustic profile as loads are applied and removed. And while it is impossible to know exactly what loads are being applied to the panels, they will change in terms of the acoustic data produced. After a time elapses and the data seems to show a more constant data set, then it could be compared on larger increments. This will allow for small changes to be examined without taking up a large part of the researcher’s time. However, the data from the monitor should still be examined on normal short intervals to look for any hits or events that are unusual, as they may be an indication of a sudden incident of possible failure activity.

References

Bayareahouston.com. (n.d.). Retrieved from http://www.bayareahouston.com/

BRE and Trend 2000 Ltd. (2001). *Polymer composites as construction materials*. Retrieved June 21, 2008, from http://www.polymercomposites.co.uk/pdf/Bridges.PDF

Ely, T.M., & Hill, E. (1995). Longitudinal splitting and fiber breakage characterization in graphite epoxy using acoustic emission data. *Materials Evaluation, 53*(2), 288-294.

Feng, P., Ye, L., Li, T., & Ma, Q. (2006). Outside filament-wound reinforcement: A novel configuration for FRP bridge decks. *The Ninth International Symposium on Structural Engineering for Young Experts, August 18-21 2006, Fuzhou & Xiamen, China*.

Gostautas, R.S., Ramirez, G., Peterman, R.J., & Meggers, D. (2005). Acoustic emission monitoring and analysis of glass fiber-reinforced composites bridge decks. *Journal of Bridge Engineering, 10*(6), 713-721.

Kansas Structural Composites, Inc. (KSCI). (2007). *Kansas Structural Composites, Inc., website*. Retrieved January 30, 2008, from http://www.ksci.com/frpbridges.html

Kawamoto, S., & Williams, R.S. (2002). *Acoustic emission and acousto-ultrasonic techniques for wood and wood-based composites: A review* (General Technical Report FPL−GTR−134). Madison, WI: U.S. Department of Agriculture, Forest Service, Forest Products Laboratory.

Kowalik, A. (n.d.). *Acoustic monitoring on the Fred Hartman Bridge*. Retrieved January 15, 2008, from ftp://ftp.dot.state.tx.us/pub/txdot-info/library/pubs/bus/bridge/hartman_acoustic_monitoring.pdf

Lanzara, G., Zhang, L., & Chang, F.K. (n.d.). *Multifunctional piezoelectric actuators (MPZT) with carbon nanotubes*. Stanford, CA: Structures and Composites Laboratory, Stanford University. Retrieved June 6, 2008, from http://structure.stanford.edu/Project/ResearchProjects/giulia/PZT%20poster%20giulia.pdf

Liu, W., Zhou, E., & Wang, Y. (2012). *Response of No-Name Creek FRP bridge to local weather* (Report No. FHWA-KS-12-6). Topeka, KS: Kansas Department of Transportation.

McWilliam, F. (1994, July 21). *Building bridges from old to new*. Retrieved June 21, 2008, from http://www.contractjournal.com/Articles/1994/07/21/30679/building-bridges-from-old-to-new.html

Prine, D.W. (1995). *Application of acoustic, strain, and optical sensors to NDE of steel highway bridges*. Retrieved January 15, 2008, from http://www.iti.northwestern.edu/publications/REG/Prine-1995-Application_of_Acoustic_Strain_and_Optical_Sensors_to_NDE_of_Steel_Highway_Bridges.pdf

Sison, M., Duke, J.C., Jr., Clemeña, G., & Lozev, M.G. (1996). Acoustic emission: A tool for the bridge engineer. Materials Evaluation, 54(8), 888-900.

Uppal, A.S., Stone, D., & Kristan, J. (2000). Monitoring bridge components using acoustic emissions. *Railway Track and Structures*, *96*(9), 22-25.

Walker, J.L., & Workman, G.L. (1998). *Study acoustic emission from composites*. Washington. D.C.: National Aeronautics and Space Administration (NASA).

Zhou, E., Wang, Y., Meggers, D., & Plunkett, J. (2007). Field tests to determine static and dynamic response to traffic loads of fiber-reinforced polyester No-Name Creek Bridge. *Transportation Research Record, 2028*, 231-237.

AD ASTRA PER ASPERA

Kansas

Department of Transportation